

2015

Oxygenation properties and isoform diversity of snake hemoglobins

Jay F. Storz

University of Nebraska-Lincoln, jstorz2@unl.edu

Chandrasekhar Natarajan

University of Nebraska-Lincoln, chandrasekhar.natarajan@unl.edu

Hideaki Moriyama

University of Nebraska-Lincoln, hmoriyama2@unl.edu

Federico G. Hoffmann


Mississippi State University, federico.g.hoffmann@gmail.com

Tobias Wang

Aarhus University, tobias.wang@bios.au.dk

See next page for additional authors

Follow this and additional works at: <http://digitalcommons.unl.edu/bioscistorz>

 Part of the [Ecology and Evolutionary Biology Commons](#), [Molecular Biology Commons](#), [Molecular Genetics Commons](#), and the [Systems and Integrative Physiology Commons](#)

Storz, Jay F.; Natarajan, Chandrasekhar; Moriyama, Hideaki; Hoffmann, Federico G.; Wang, Tobias; Fago, Angela; Malte, Hans; Overgaard, Johannes; and Weber, Roy E., "Oxygenation properties and isoform diversity of snake hemoglobins" (2015). *Jay F. Storz Publications*. 64.

<http://digitalcommons.unl.edu/bioscistorz/64>

This Article is brought to you for free and open access by the Papers in the Biological Sciences at DigitalCommons@University of Nebraska - Lincoln. It has been accepted for inclusion in Jay F. Storz Publications by an authorized administrator of DigitalCommons@University of Nebraska - Lincoln.

Authors

Jay F. Storz, Chandrasekhar Natarajan, Hideaki Moriyama, Federico G. Hoffmann, Tobias Wang, Angela Fago, Hans Malte, Johannes Overgaard, and Roy E. Weber

Oxygenation properties and isoform diversity of snake hemoglobins

Jay F. Storz,¹ Chandrasekhar Natarajan,¹ Hideaki Moriyama,¹ Federico G. Hoffmann,^{2,3}
Tobias Wang,⁴ Angela Fago,⁴ Hans Malte,⁴ Johannes Overgaard,⁴ and Roy E. Weber⁴

¹ School of Biological Sciences, University of Nebraska–Lincoln, Lincoln, Nebraska

² Department of Biochemistry, Molecular Biology, Entomology, and Plant Pathology, Mississippi State University, Starkville, Mississippi

³ Institute for Genomics, Biocomputing, and Biotechnology, Mississippi State University, Mississippi State, Mississippi

⁴ Zoophysiology, Department of Bioscience, Aarhus University, Aarhus, Denmark

Corresponding author — J. F. Storz. School of Biological Sciences, University of Nebraska–Lincoln, 1400 R St., Lincoln, NE 68588; email jstorz2@unl.edu

Abstract

Available data suggest that snake hemoglobins (Hbs) are characterized by a combination of unusual structural and functional properties relative to the Hbs of other amniote vertebrates, including oxygenation-linked tetramer-dimer dissociation. However, standardized comparative data are lacking for snake Hbs, and the Hb isoform composition of snake red blood cells has not been systematically characterized. Here we present the results of an integrated analysis of snake Hbs and the underlying α - and β -type globin genes to characterize 1) Hb isoform composition of definitive erythrocytes, and 2) the oxygenation properties of isolated isoforms as well as composite hemolysates. We used species from three families as subjects for experimental studies of Hb function: South American rattlesnake, *Crotalus durissus* (Viperidae); Indian python, *Python molurus* (Pythonidae); and yellow-bellied sea snake, *Pelamis platura* (Elapidae). We analyzed allosteric properties of snake Hbs in terms of the Monod-Wyman-Changeux model and Adair four-step thermodynamic model. Hbs from each of the three species exhibited high intrinsic O_2 affinities, low cooperativities, small Bohr factors in the absence of phosphates, and high sensitivities to ATP. Oxygenation properties of the snake Hbs could be explained entirely by allosteric transitions in the quaternary structure of intact tetramers, suggesting that ligation-dependent dissociation of Hb tetramers into $\alpha\beta$ -dimers is not a universal feature of snake Hbs. Surprisingly, the major Hb isoform of the South American rattlesnake is homologous to the minor HbD of other amniotes and, contrary to the pattern of Hb isoform differentiation in birds and turtles, exhibits a lower O_2 affinity than the HbA isoform.

Keywords: allosteric regulation, blood-oxygen transport, *Crotalus*, *Pelamis*, python

Snakes inhabit an extensive range of terrestrial and aquatic environments and experience a wide range of metabolic responses to varying environmental conditions, physiological states, and levels of physical activity. The variation in tissue O_2 demand in snakes is compounded by drastic postprandial increases in aerobic metabolism, episodic breathing, bimodal (pulmonary and cutaneous) respiration, and large variations in body temperature (which affect both metabolism and blood O_2 affinity) and anaerobic metabolism (12, 30, 48, 57, 62–64, 67, 71, 78). Compared with the extensive data on the hemoglobins (Hbs) of other vertebrate taxa, little is known about the molecular mechanisms that underlie HbO_2 transport in snakes.

The Hbs of jawed vertebrates are heterotetramers, composed of paired, semirigid $\alpha\beta$ -dimers that undergo a symmetrical rotation during ligation transitions in quaternary structure. This $\alpha_2\beta_2$ quaternary structure is central to both homotropic allostery (cooperative binding of O_2 to the heme iron of each globin subunit) and heterotropic allostery (regulation of heme O_2 affinity by binding nonheme ligands at structurally distinct sites) (5, 7, 60). Both forms of allostery are mediated by a conformational equilibrium between high- and low-affinity quaternary structures (the “R” and “T” states, respectively). The main mechanism of heterotropic allostery involves preferential binding of H^+ , Cl^- , CO_2 , and/or organic phosphates to deoxygenated Hb (deoxy-Hb), which stabilizes the T-state conformation and shifts the allosteric equilibrium in favor of this low O_2 affinity quaternary structure. Although allosteric regulation of O_2 binding is a fundamental feature of vertebrate Hbs, O_2 affinity within the red cell is regulated by different organic phosphate ef-

factors in different taxa (6, 13, 40, 52, 65, 82, 86, 92). ATP is the main organic phosphate within the red cells of most squamates (lizards and snakes), but the red cells of snakes may also contain substantial levels of guanosine triphosphate (GTP), as commonly found in fish erythrocytes (6, 54).

Among amniotes, snakes appear to possess Hbs with a combination of unusual properties. Available data for several species suggest that snake Hbs are generally characterized by high O_2 affinities, low cooperativities, and low pH sensitivities relative to the Hbs of other amniotes (9–11, 18, 24, 26, 44, 45, 47, 53, 54, 69, 76). Interestingly, results of in vitro studies suggest that Hbs of several snake species undergo oxygenation-linked dissociation of tetramers into $\alpha_1\beta_1$ - and $\alpha_2\beta_2$ -dimers in the absence of organic phosphates and at high pH (9, 24–26, 47, 53, 54, 58). These findings suggest that ATP may regulate HbO_2 affinity, not only by shifting the allosteric equilibrium between R- and T-state quaternary structures, but also by inhibiting tetramer-dimer dissociation. Some authors have suggested that reversible, oxygenation-linked tetramer-dimer dissociation is a general feature of Hbs in ectothermic vertebrates that may represent a retained ancestral character state (9). Although the O_2 affinity of snake Hb is greatly reduced and the alkaline Bohr effect is greatly enhanced in the presence of ATP (11, 44, 45), these effects could possibly stem from ATP-induced polymerization of subunits. However, experimental studies of purified Hbs from the South American rattlesnake (*Crotalus durissus*) and common water snake (*Lio-phis miliaris*) revealed that intact tetrameric assemblies predominated even at exceedingly low Hb concentrations, and tetramer-

dimer dissociation rate constants were actually lower than those of human Hb (44, 45). These results suggest that oxygenation-linked tetramer-dimer dissociation is not a universal feature of snake Hbs, and that it is unlikely to be physiologically relevant *in vivo* (10).

Oxygenation properties have been characterized for the Hbs of several snake species (reviewed by Refs. 13, 40, 86), but little is known about structure-function relationships due to the dearth of sequence data and the absence of any crystallographic data for snake Hbs. Likewise, little is known about Hb isoform (isoHb) diversity in the red blood cells of snakes or other squamate reptiles. Most studies report the existence of two or more structurally distinct isoHbs in the definitive erythrocytes of snakes (10, 20, 21, 26, 44, 45, 58, 76), but it is not always clear to what extent the apparent isoHb diversity reflects ligation- and/or oxidation-dependent changes in quaternary structure.

During postnatal life, birds, lizards, and turtles typically express two main isoHbs that incorporate structurally distinct α -type subunits: HbA, which incorporates products of the α^A -globin gene, and HbD, which incorporates products of the α^D -globin gene (17, 31, 55, 72). Since the duplicative origins of the α^A - and α^D -globin genes predate the radiation of tetrapod vertebrates (37, 38, 72–74), snakes may also express homologs of the HbA and HbD isoforms that have been described in other tetrapods. If so, it would be of interest to determine whether the two isoHbs have retained the same characteristic differences in functional properties that have been documented in turtles (17) and birds (15, 27, 31, 33, 34, 61). Given that some snakes are known to possess multiple α - and/or β -globin gene duplicates (28, 38), it is also possible that snakes express isoHbs that represent previously undescribed combinations of distinct α - and β -type subunits.

Here we present the results of an integrated analysis of snake Hbs and the underlying globin genes to characterize **1)** the isoHb composition of definitive erythrocytes, and **2)** the oxygenation properties of isolated isoHbs as well as composite hemolysates. We used species from three families as subjects for experimental studies of Hb function: South American rattlesnake, *Crotalus durissus* (Viperidae); Indian python, *Python molurus* (Pythonidae); and yellow-bellied sea snake, *Pelamis platurus* (Elapidae). These phylogenetically disparate taxa encompass a broad range of variation with respect to natural history and ecological physiology.

We address the following questions. What is the mechanistic basis of the high O₂ affinity, low cooperativity, and attenuated Bohr effect that appear to be characteristic of snake Hbs? Can these properties be explained by allosteric transitions in the quaternary structure of intact tetramers, or are they primarily attributable to oxygenation-linked tetramer-dimer dissociation? What is the nature of isoHb differentiation? Is the isoHb repertoire of snakes qualitatively similar to that of other amniotes, or have they retained distinct components of the ancestral globin repertoire of reptiles? By integrating the structural and functional data with a phylogenetic analysis of globin sequences from snakes and other amniotes, we are able to interpret our findings in an evolutionary framework.

Materials and Methods

Experimental animals were handled in accordance with protocols approved by the Danish Animal Inspectorate.

Molecular Cloning and Sequencing

To characterize structural variation of snake Hbs, we obtained complete nucleotide or amino acid sequences of the adult-expressed α - and β -type globin genes of 23 squamate reptile species (19 snakes and 4 lizards). For the South American rattlesnake (*C. durissus*), we sequenced globin cDNAs after isolating RNA from definitive red blood cells. For the remaining species, we obtained globin sequences from public databases, or we annotated globin sequences from genome assemblies.

In the case of the South American rattlesnake, we extracted total RNA from washed red blood cells using the RNeasy mini kit (Qiagen, Valencia, CA). We used an alignment of adult-expressed globin genes and flanking untranslated regions (5' and 3' untranslated regions) from *Crotalus adamanteus* to design paralog-specific PCR primers, and we then used reverse-transcriptase (RT) PCR to amplify complete cDNAs of each α -type globin gene in *C. durissus* (One Step RT-PCR kit; Qiagen, Valencia, CA). To amplify and sequence the β -type globin genes of *C. durissus*, we first used RACE-PCR to obtain sequence information for the 5' and 3' untranslated regions of each gene, and, after designing paralog-specific primers, we then used RT-PCR to amplify complete cDNAs. RT-PCR and RACE-PCR primer sequences are provided in Table 1. We cloned gel-purified RT-PCR products into the pCR4-TOPO vector (Invitrogen Life Technologies). The cloned RT-PCR products were then sequenced on an ABI 3730 capillary sequencer using Big Dye chemistry (Applied Biosystems, Foster City, CA). DNA sequences were deposited in GenBank under the accession nos. KT438559–KT438561.

Sequence Alignment and Phylogenetic Analysis

Nucleotide sequences of the globin genes were conceptually translated into amino acid sequences using MEGA version 6.06 (78). After the α - and β -type globin sequences were aligned using muscle (19), we used MEGA to estimate maximum likelihood phylogenies under a WAG+ Γ model of amino acid substitution with five different site categories. Support for all nodes was evaluated with 1,000 bootstrap pseudoreplicates. In the phylogeny reconstruction of α -type globin genes, we included sequences from additional amniote outgroups, since the α^E -, α^D -, and α^A -globin genes are known to have originated via duplication events that occurred before the radiation of tetrapods (37, 38, 72).

Hb Sample Preparation and Protein Purification

In the case of the South American rattlesnake, blood was drawn from two animals (~450 g), and red cells were washed twice in saline and frozen at –80°C until use. The thawed material was centrifuged for 10 min at 14,000 rpm to remove cellular debris. Hb was “stripped” of organic phosphates by twice passing Hb samples through MB-1 ion exchange resin that had been rinsed with distilled water. The hemolysate was centrifuged for 2 min at 3,200 rpm, and the sample was then saturated with CO, dialyzed

Table 1. RT-PCR and RACE-PCR primers used to amplify adult-expressed α - and β -type globin genes of the South American rattlesnake (*Crotalus durissus*)

Gene	Primer Name	Sequence
α^A	5'UTR_HBA	5'-CCCTCCATCTCCTTCTCTACCACGACC-3'
	3'UTR_HBA	5'-GGGCCCCCGTTGTAGCACGTGGAGC-3'
α^D	5'UTR_HBD	5'-CAGCTATCGAGGGCAGCAACCCGCCAAG-3'
	3'UTR_HBD	5'-GGTCATTATTTCCGAGCACAGGCAGGG-3'
β	RACE_HBBExon1	5'-ATGGTGCASTGGACSSCCGARGAGAAG-3'
	RACE_HBBExon3	5'-GTGGTACCGTGGGCCAAGGCGTGGC-3'
	RACE_HBBExon2	5'-CGCTCAGCTTGGCGAAGGTGTCC-3'
	3'UTR_HBB	5'-GAAGGCGCGGCCGAGCCGCTGCGGA-3'
	5'UTR_HBB	5'-GACACCTTCGCCAAGCTGAGCGAAGGGC-3'

against three changes of 0.01 M HEPES buffer, pH 7.6, containing 0.5 mM EDTA (dialysis buffer), and recentrifuged (2 min at 3,200 rpm). All preparative procedures were carried out at 0–5°C. Samples from both specimens were pooled for O₂-equilibrium measurements.

Ion exchange chromatography was carried out at 5°C on a 23.4 × 2 (height × diameter) column of DEAE Sephacel eluted with a linear gradient of 0 to 0.15 M NaCl (in 0.02 M Tris buffer, pH 8.4, at 5°C). Isolated Hb fractions were dialyzed against dialysis buffer (as above) and concentrated by ultrafiltration on Millipore Ultrafiltration membranes filters (PLGC 02500) with a 10-kDa cutoff. Hemolysate and fractionated Hb preparations were frozen at –80°C in 100- to 150-μl aliquots that were thawed individually before measuring O₂ equilibria. Electrophoresis on cellulose acetate strips was carried out on Millipore Phorolide system (30 min runs, at 100 V). SDS polyacrylamide gel electrophoresis was carried out in the presence and absence of β-mercaptoethanol in the sample buffer, as previously described (23).

Gel filtration experiments were carried out on a 59.3 × 2.6 cm column of Sephacryl S200 HR. The Hbs were eluted with 0.025 M Tris (pH 7.4) containing 0.025 M NaCl and 0.003 M sodium azide. Gel filtration of deoxy-Hb was carried out by adding sodium dithionite (1 mg/ml) to the previously N₂-equilibrated elution buffer (pH 6.75), using Hb samples that

had not been in contact with CO. The absence of free oxygen in these runs was confirmed with a Radiometer (Copenhagen) O₂ electrode (type E5046) and thermostated cell (type D616) connected to the column outlets. The molecular masses of oxygenated and deoxygenated rattlesnake Hb were estimated by comparing their partition coefficients, $K_{AV} = [(V_e - V_0)/(V_t - V_0)]$, where V_e is the elution volume, V_0 is the void volume, and V_t is the total volume of gel] with the corresponding values obtained for proteins of known molecular mass, including human Hb, cytochrome-c, sperm whale myoglobin, oval albumin, bovine serum albumin, aldolase, and ferritin (84).

The Indian python and yellow-bellied sea snake Hbs were purified using a protocol similar to that used for the rattlesnake Hbs, except that the red cells were lysed by freezing at –80°C combined with osmotic shock, and *P. molurus* Hb was “stripped” by column chromatography on Sephadex G25 Fine gel equilibrated with 50 mM Tris buffer, pH 7.8, containing 0.1 M NaCl (84). In each species, Hb was purified from the blood sample of a single adult individual.

Molecular weight measurements of python oxy-, deoxy-, and carboxy-Hbs were performed at room temperature (~25°C) in the absence or presence of 1 mM ATP, using a column of Superose 12HR10/30 equilibrated with 0.1 M HEPES elution buffer, pH 7.1, connected to a Waters FPLC

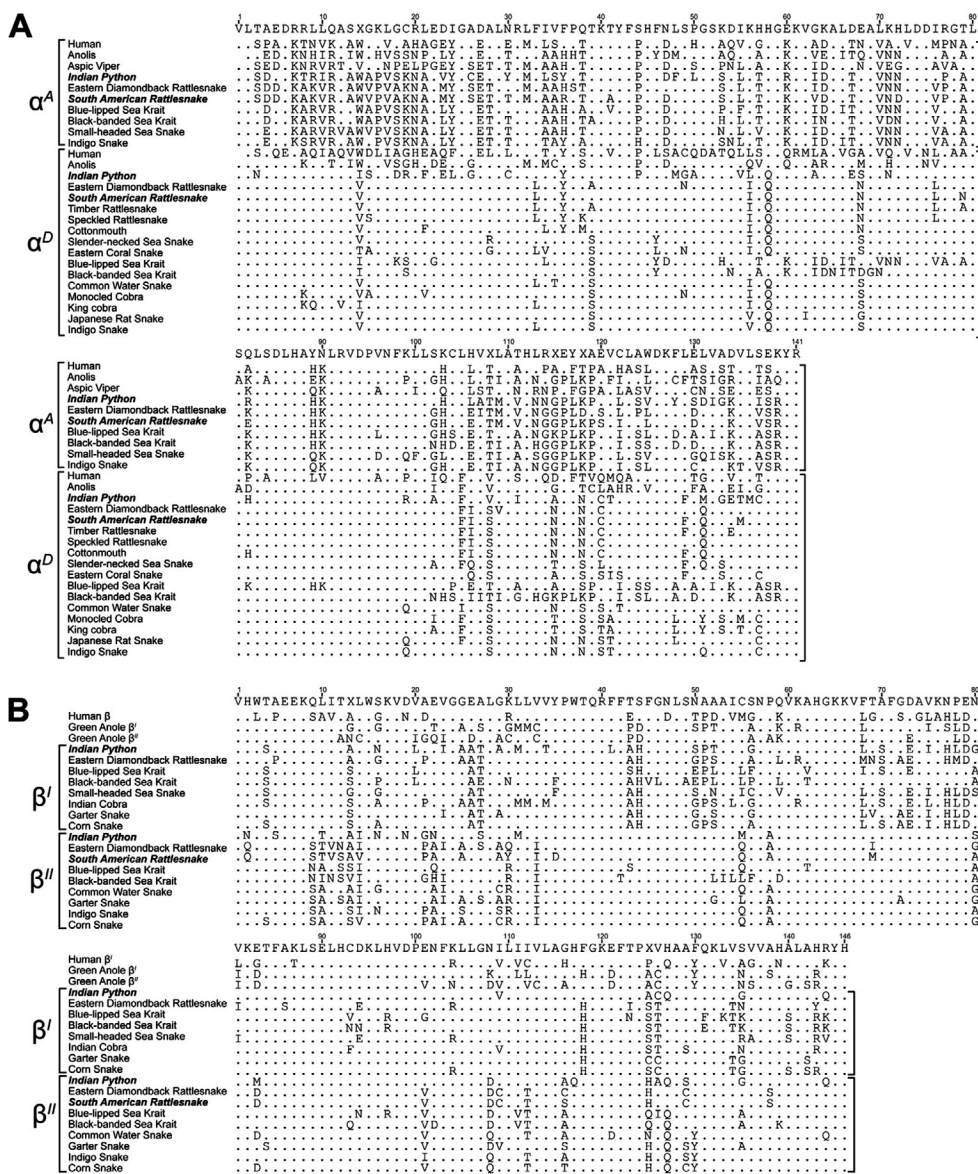


Figure 1. Alignment of amino acid sequences representing the complete repertoire of adult-expressed α- (A) and β- type globin genes (B) from snakes and two outgroup taxa: human (*Homo sapiens*) and green anole lizard (*Anolis carolinensis*). Names of species included in the functional studies [South American rattlesnake (*Crotalus durissus*) and Indian python (*Python molurus*)] are in bold.

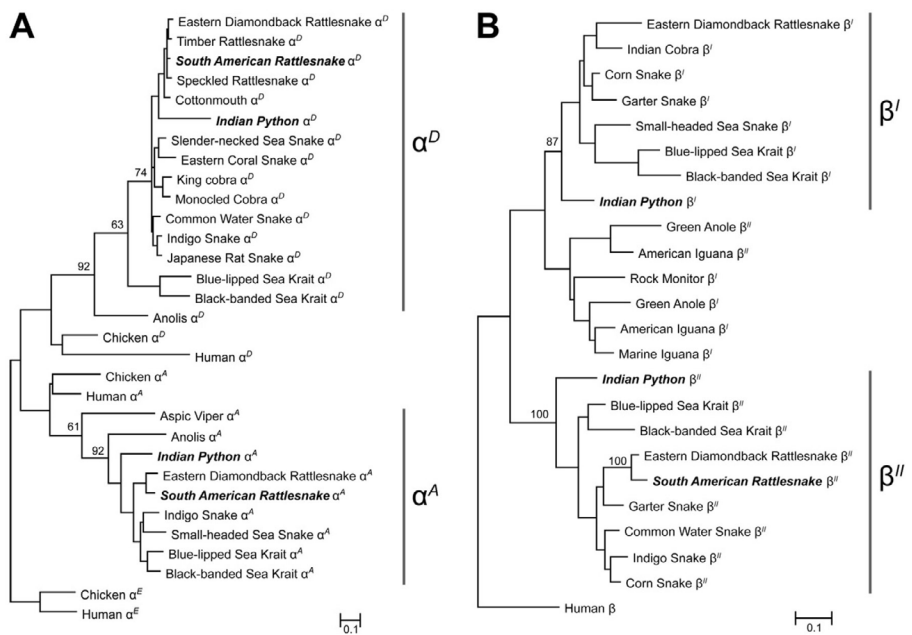


Figure 2. Phylogeny of α - (A) and β -type globin genes (B) of snakes, including the full set of adult-expressed α - and β -type globin genes from South American rattlesnake (*Crotalus durissus*) and Indian python (*Python molurus*). Separate phylogenies for α -type and β -type globin genes are shown.

analyzer (Milford, MA) and eluted at a flow rate of 0.4 ml/min. The column was calibrated with sperm whale myoglobin (mass 17 kDa) and the cathodic isoHb component I of trout (molecular mass 64 kDa), which is a more stable Hb tetramer than human Hb (14). Deoxygenation was obtained by addition of sodium dithionite (1 mg/ml) to elution buffer equilibrated with pure N_2 and was monitored from absorbances at 555 nm and 540 nm [approximate absorbance peaks of deoxy-Hb and oxygenated Hb (oxy-Hb), respectively]. As ligated Hb, we used HbCO, which is a more stable derivative than oxy-Hb. The applied sample was ~0.5 mM heme, resulting in an end concentration of ~0.2 mM heme (46). Thin-layer isoelectrofocusing of python Hb was carried out in a 3.5–10 pH range on 0.3-mm-thick 7.5% polyacrylamide gels using the Multiphor II flatbed electrophoresis system (Pharmacia, Uppsala, Sweden).

IsoHb Composition of Rattlesnake Red Cells

After using anion exchange chromatography to resolve the rattlesnake hemolysate into separate Hb components, we identified the subunit composition of each tetrameric $\alpha_2\beta_2$ isoHb by using a combination of cDNA sequencing, NH_2 -terminal peptide sequencing, and tandem mass spectrometry (MS/MS). For the NH_2 -terminal peptide sequencing, individual α - and β -chain subunits of the purified Hb components were separated by means of 20% SDS-PAGE. After staining with Coomassie brilliant blue, the gel was transferred to a 0.2- μ m nitrocellulose membrane. The protein was recovered from the membrane and was then subjected to peptide sequencing, as described previously (50). For the MS/MS analysis, the α - and β -globin chains were separated by means of 20% SDS-PAGE, and the gel bands were then excised and digested with trypsin. Specifically, peptide mass fingerprints derived from the MS/MS analysis were used to query a custom database on the Mascot data search system (Matrix Science, version 1.9.0, London, UK) that included amino acid sequences from all adult-expressed α - and β -type globin genes of *C. durissus* and other snake species, in addition to the full complement of pre- and postnatally expressed α - and β -type globin genes that have been annotated from other amniote vertebrates (35, 36, 38, 55, 72, 94). The following search parameters were used for the MS/MS analysis: no restriction on protein molecular weight or isoelectric point, and methionine oxidation allowed as a variable peptide modification. Mass accuracy settings were 0.15 Da for peptide mass and 0.12 Da for fragment ion masses. We identified all significant protein hits that matched more than one peptide with $P < 0.05$.

Measurement of HbO₂ Equilibria

We measured O_2 -equilibrium curves for stripped hemolysates (and isolated isoHbs of rattlesnake) using a modified gas diffusion chamber coupled to cascaded Wösthoff pumps for mixing pure N_2 (>99.998%), O_2 , and atmospheric air (31, 51, 66, 75, 84, 85). Changes in the absorbance spectra of thin-layer Hb solutions (4 μ l) were measured following stepwise changes in the partial pressure of O_2 (P_{O_2}) inside the chamber. Values of P_{50} (the P_{O_2} at which Hb is 50% saturated with O_2) and n_{50} (Hill's cooperativity coefficient at 50% saturation) were interpolated from linear plots of $\log [Y/(Y - 1)]$ vs. $\log P_{O_2}$ for at least four saturation values between 25 and 75%. Using this method, the r^2 determination coefficient for the fitted curve typically exceeds 0.995 (83).

To assess HbO₂ affinities and the sensitivities to allosteric effectors, we measured O_2 equilibria of “stripped” cofactor-free Hbs in 0.10 M Cl^-

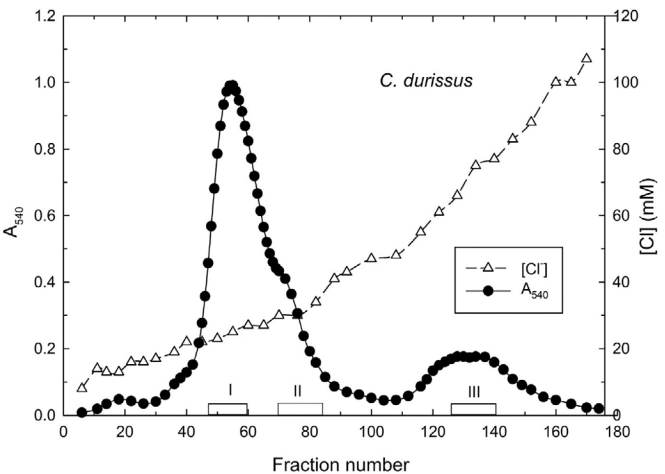


Figure 3. Anion exchange chromatography elution profile of rattlesnake hemoglobin (Hb) performed on DEAE Sephacel gel. Bars I, II, and III indicate the fractions pooled for O_2 -equilibrium measurements. A_{540} , absorbance at 540 nm; $[Cl^-]$, concentration of Cl^- .

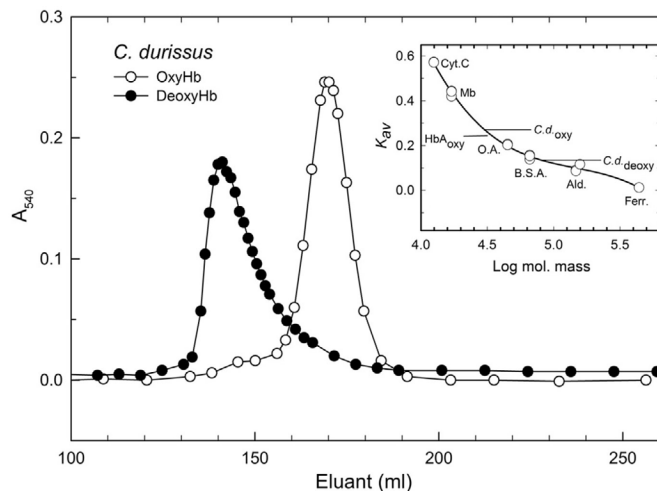


Figure 4. Chromatography profiles showing higher elution volume of oxygenated (oxy-Hb; ○) compared with deoxygenated Hb (deoxy-Hb; ●) of South American rattlesnake (*C. durissus*), observed in gel filtration analysis on Sephacryl S-200 HR gel (see materials and methods). *Inset:* partition coefficient K_{AV} values for oxygenated and deoxygenated rattlesnake Hbs (Cd_{oxy} and Cd_{deoxy} , respectively) and oxygenated human Hb (HbA_{oxy}), compared with the values for proteins of known molecular mass: cytochrome c (Cyt C), sperm whale myoglobin (Mb), oval albumin (OA), bovine serum albumin (BSA), aldolase (Ald), and ferritin (Ferr).

(added as KCl) and 0.10 M Na-HEPES buffers, in the absence and the presence of organic phosphates at different phosphate-to-Hb ratios, and at heme concentrations of 0.04–0.30 mM (as indicated). The temperature sensitivity of P_{50} is indexed in terms of the overall (apparent) enthalpy of oxygenation, $\Delta H'$, calculated using the van't Hoff isochore: $\Delta H' = 2.303R \cdot \Delta \log P_{50} / \Delta(1/T)$ (93), where R is the gas constant, and T is the absolute temperature.

For stripped rattlesnake and python Hbs, we conducted detailed analyses of allosteric interactions based on measurements of O_2 equilibria that included extremely high and extremely low saturation values. This allowed us to analyze the data in terms of the two-state Monod-Wyman-Changeux (MWC) allosteric model (49), which relates HbO_2 saturation (Y) to the P_{O_2} (P), the O_2 association equilibrium constants for “R-state” oxy-Hb and “T-state” deoxy-Hb (K_R and K_T , respectively), the allosteric constant (L , the

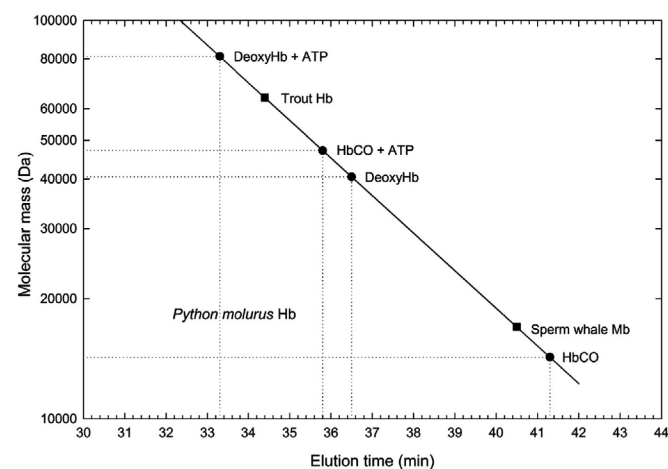


Figure 5. Elution times for gel filtration of deoxy-Hb and carboxylated Hb (HbCO) of the Indian python (*P. molurus*) on a Superose column, compared with the values for trout Hb and sperm whale Mb of known molecular mass.

ratio of T- and R-state Hb in the absence of ligand), and the number of interacting O_2 binding sites (q):

$$Y = \frac{LK_T P(1 + K_T P)^{q-1} + K_R P(1 + K_R P)^{q-1}}{L(1 + K_T P)^q + (1 + K_R P)^q}$$

Measures of $\log[Y/(1 - Y)]$ as a function of $\log P_{O_2}$ were fitted to the model by means of nonlinear least squares regression using the Levenberg-Marquardt method, as implemented in Mathematica (version 5.2, Wolfram Research, Champaign, IL). Corrections due to errors arising from incomplete saturation and desaturation were calculated as described by Fago et al. (22), and estimates of standard errors for the fitted parameters were obtained as described by Weber et al. (89).

In separate analyses, values of q were either fitted freely along with the other parameters, or were fixed at 4, as applies to tetrameric Hb. The two-state MWC parameters derived for $q = 4$ were used to calculate the intrinsic Adair constants that characterize the affinities of four successive heme oxygenation steps (2). Several parameters, including median O_2 tension (P_m), median cooperativity coefficient (n_m), and the free energy of cooperativity (ΔG) were calculated as previously described (88). Analysis of effector and temperature sensitivities of the snake Hbs in terms of variations in P_{50} is justified by the agreement between P_{50} and P_m and between n_{50} and n_m values, which reflects overall symmetry of the O_2 binding curves (3).

Results

Structural Variation of Snake Hbs

Alignment of adult α - and β -type globin genes from a phylogenetically diverse set of squamate reptiles revealed that snakes typically possess multiple genes encoding each subunit type (Figure 1). To infer the orthologous and paralogous relationships of these globin sequences, we reconstructed phylogenetic relationships using alignments that included globin sequences from additional amniote outgroup taxa (Figure 2). The phylogeny reconstructions revealed that snakes typically possess a repertoire of four

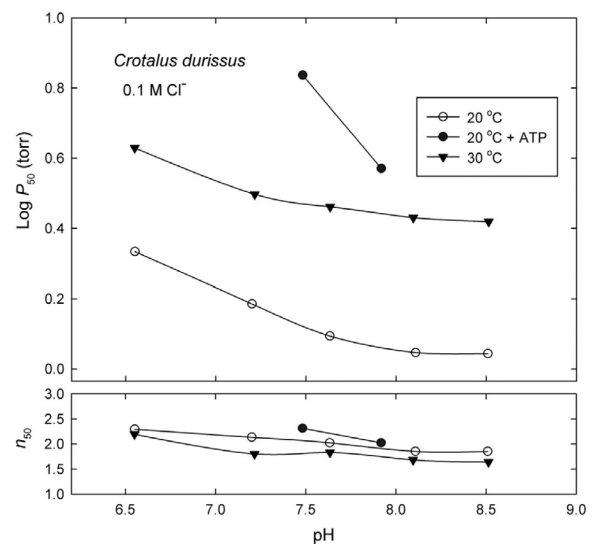


Figure 6. O_2 tensions (P_{50}) and Hill's cooperativity coefficients at half-saturation (n_{50}) of stripped hemolysate of the South American rattlesnake (*C. durissus*). Plots show pH dependence of HbO_2 affinity and cooperativity, measured at 20°C (circles) and 30°C (inverted triangles) in the presence of 0.1 M KCl and 0.1 M HEPES buffers, and in the absence (open symbols) and presence (solid symbols) of saturating ATP concentrations (molar ATP-to-tetrameric Hb ratio ~60). Heme concentration, 0.32 mM.

Table 2. O₂-affinity of stripped snake Hbs, as indexed by P₅₀ values, the pH sensitivity of O₂ affinity, as indexed as Bohr factors (Δlog P₅₀/ΔpH, at pH 7.0–7.4), and ATP sensitivity of O₂ affinity, as indexed by the difference in log-transformed P₅₀ values measured in the presence and absence of ATP

	P ₅₀ , Torr		ΔLog P _{50(ATP-str)}	Experimental Conditions					Bohr Factor (pH ~7.0–7.4)		
	Str.	Str. + ATP		°C	pH	Buffer	[Cl ⁻]	[Heme], mM	Str.	Str. + ATP	Ref. No.
<i>Crotalus durissus</i>											
Hemolysate	1.4	7.7	0.74	20	7.4	0.1 M HEPES	0.1 M KCl	0.32	-0.21	-0.62	This study
Hb I	1.2	4.6	0.58	20	7.4	0.1 M HEPES	0.1 M KCl	0.04	-0.14	-0.56	This study
Hb II	0.8	2.1	0.42	20	7.4	0.1 M HEPES	0.1 M KCl	0.04	-0.07	-0.47	This study
Hb III	0.4	1.3	0.51	20	7.4	0.1 M HEPES	0.1 M KCl	0.04	-0.13	-0.49	This study
<i>Crotalus durissus terrificus</i>	1.0	4.9	0.69	20	7.5	0.05M Tris/HEPES	0.1 M NaCl	0.05	-0.60		44
<i>Python molurus</i>	1.0	2.9	0.46	25	7.4	0.1 M HEPES	0.1 M KCl	0.20	-0.17	-0.66	This study
<i>Pelamis platura</i>	1.2	4.5	0.57	25	7.4	0.1 M HEPES,	0.1 M KCl	0.20	-0.17	-0.56	This study
<i>Boa constrictor</i>	0.8	6.3	0.89	25	7.5	0.05 M Tris		0.06	0	-0.60	24
<i>Boa constrictor amarali</i>											
Hb SS	0.71	2.33	0.52	20	7.4	0.1 M Tris		?	-0.25	-0.76	68
Hb SF	0.93	2.33	0.40	20	7.4	0.1 M Tris		?	-0.21	-0.76	68
<i>Mastigodryas bifossatus</i> hemolysate	1.3	12.60	0.99	20	7.4	0.05 M Bis-Tris		0.05	-0.30		10
Hb I	1.2			20	7.1	0.05 M Bis-Tris		0.05			10
Hb II	1.5			20	7.1	0.05 M Bis-Tris		0.05			10
<i>Mastigodryas bifossatus</i>											
<i>Liophis miliaris</i>	1.04	10.9	1.02	25	7.4	0.05 M Tris		0.44	-0.30	-0.90	52
<i>Helicops modestus</i>	0.95	5.7	0.78	25	7.4	0.05 M Tris		0.44	-0.07	-0.55	52
<i>Bothrops alternatus</i>	1.0	7.2	0.86	20	7.5	0.2 M Tris		0.06	-0.38	-0.69	52
Hb I	1.2	7.2	0.78	20	7.5	0.2 M Tris		0.06	-0.38	-0.69	
Hb II	1.0	5.0	0.70	20	7.5	0.2 M Tris		0.06	-0.38	-0.69	
Human	3.98			25	7.4	0.1 M HEPES	0.1 M KCl	0.40			10
Human	5.32	14.0 ^a	0.42 ^a	25	7.4	0.05 M Bis-Tris	0.1 M KCl	0.60	-0.51	-0.63 ^a	39

Data for human hemoglobins (Hbs) are shown for comparison. P₅₀ = the Po₂ at which Hb is 50% saturated with O₂; Str = stripped; [Cl⁻] = Cl⁻ concentration; [Heme] = heme concentration; Δlog P_{50(ATP-str)} = difference in log-transformed P₅₀ values measured in the presence and absence of ATP.

a. Values for human Hbs were measured in the presence of 2,3-diphosphoglycerate (instead of ATP, as in the experiments involving snake Hbs).

adult-expressed globin genes, including single copies of α^A- and α^D-globin, and two β-globin gene duplicates, β^I and β^{II} (38). The phylogeny of squamate β-type globins indicates that the β^I- and β^{II}-globin genes of snakes are products of a duplication event that occurred before the divergence of snakes and lizards, as all lizard genes are sister to the clade of snake β^I-globins; orthologs of snake β^{II}-globin appear to have been secondarily lost in lizards (Figure 2B). In the South American rattlesnake, the presence of premature stop codons clearly indicates that β^{II} is a pseudogene. The ortholog of this same gene has an open reading frame in the closely related eastern diamondback rattlesnake, *Crotalus adamanteus* (Figure 1).

isoHb composition—South American rattlesnake. Electrophoresis of a freshly prepared rattlesnake hemolysate on cellulose acetate strips (not shown) revealed the presence of one major anodally migrating Hb component and one minor component with slower anodal migration. Anion exchange chromatography resolved the hemolysate into one major and two minor Hb components (I, II, and III; Figure 3), and indicated three to four additional trace components. SDS-PAGE showed the same molecular mass of subunits (~13–13.5 kDa) in the presence and absence of reducing agent, indicating the absence of disulphide bonds.

Mass spectrometry analysis revealed that each of the three main isoHbs share the same β-chain subunits (products of the β^{II}-globin gene). The major isoHb (component I) incorporates products of the α^D-globin gene (α^D₂β^{II}₂), and the minor component III incorporates products of the α^A-globin gene (α^A₂β^{II}₂). The minor component II appears to have the same subunit composition as com-

ponent I, suggesting that the observed charge differences between the two components may be attributable to deamination or some other form of posttranslational modification.

isoHb composition—Indian python. Thin layer isoelectric focusing of python hemolysate showed three bands with nearly identical isoelectric point values between pH 7.65 and 7.85. Accordingly, we did not attempt to separate individual isoHbs.

isoHb composition—yellow-bellied sea snake. Electrophoresis and anion exchange chromatography of sea snake hemolysate revealed the presence of two major Hb fractions that contribute ~75 and 25% of the total (not shown). Liu (43) reported that the major isoHb is a hybrid tetramer (α₂β₁β₂), where the COOH-terminal sequence of one of the two β-chains (-Arg-Leu-His-Tyr) reveals loss of the COOH-terminal His residue that contributes a major part of the Bohr effect in vertebrate Hbs.

Ligation-Dependent Changes in Hb Quaternary Structure

Changes in the quaternary structure of South American rattlesnake Hb. Gel filtration experiments revealed a distinctly higher aggregation state in deoxygenated than in the oxygenated rattlesnake Hb. Comparison of the partition coefficients (K_{AV} values) with those of other proteins of known molecular mass indicated molecular masses of 80 and 35 kDa, respectively (Figure 4). The value of 38 kDa obtained for human Hb (inset of Figure 4) is consistent with observations that molecular masses of tetrameric vertebrate Hbs obtained from gel filtration experiments are appreciably lower than the established values based on primary structures

(64–68 kDa), which may result from reversible dissociation to dimers (16) and the compact nature of tetrameric vertebrate Hbs, given that elution volumes in gel filtration are inversely related to the Stokes radii of proteins rather than molecular weights (1). It follows that the molecular mass estimates obtained under the experimental conditions indicate a tetrameric-dimeric equilibrium in oxygenated rattlesnake Hb and aggregation of the deoxygenated molecules to larger complexes (likely octameric).

Changes in the quaternary structure of Indian python Hb. Gel filtration experiments revealed marked dependence of the quaternary structure of python Hb on ligation state, the molecular masses being higher in deoxy-Hb than in HbCO in the absence of ATP (~40 and ~14 kDa, respectively) and in the presence of ATP (~81 and ~47 kDa, respectively) (Figure 5). This indicates a monomer \leftrightarrow dimer \leftrightarrow tetramer \leftrightarrow polymer equilibrium, where the low mass values reflect dissociation of ligated HbCO and oxy-Hb to monomers in the absence of ATP, and the high values reflect aggregation of deoxy-Hb to higher-order structures (larger than tetramers) in the presence of ATP.

Oxygenation Properties of Snake Hbs

The O₂-binding equilibrium properties of the Hbs of the three snake species were examined in varying levels of detail. For the purified Hbs of South American rattlesnake, Indian python, and yellow-bellied sea snake, we measured basic oxygenation properties and mechanisms of allosteric regulatory control (anion and pH sensitivity of HbO₂ affinity). In the case of rattlesnake and python, we obtained measurements of HbO₂ equilibria over a wide range of O₂ saturation values (including extremely high and low saturations), thereby permitting detailed analyses of Hb allostery in terms of the MWC model and Adair four-step thermodynamic model. In the case of rattlesnake, we measured oxygenation properties of the unfractionated hemolysate, in addition to those of the three constituent isoHbs. We present the results of O₂ binding experiments for each species in turn.

Functional properties of South American rattlesnake Hbs. The stripped, unfractionated hemolysate of the rattlesnake exhibited very high O₂ affinity (P_{50} at pH 7.4 = 1.4 Torr at 20°C) and a small Bohr effect [Bohr factor (ϕ) at pH 7.0–7.4 = –0.21 and –0.11, respectively, at 20 and 30°C; Figure 6, Table 2]. The addition of ATP drastically increased both P_{50} (to 7.8 Torr at 20°C and pH 7.4) and the ϕ (to –0.62). The P_{50} values of rattlesnake Hb at 20 and 30°C (Figure 6) reveal a high overall heat of oxygenation at high pH ($\Delta H' = -64$ kJ/mol at pH 8, where the Bohr effect is negligible) that decreases at lower pH where the Bohr effect is expressed (–52.7 kJ/mol at pH 7.0). The observed decrease in the heat of oxygenation with pH is consistent with the known endothermic liberation of bound protons upon oxygenation (80).

For rattlesnake, we also measured O₂ equilibria of fractions containing each of the three main isoHbs (Figure 7). The most abundant isoHb (component I) exhibited a similar O₂ affinity as the unfractionated hemolysate at the same Hb concentration ($P_{50} = 1.2$ at pH 7.4), whereas the remaining two isoHbs (components II and III) exhibited higher O₂ affinities ($P_{50} = 0.8$ and 0.4 Torr, respectively, at pH 7.4). None of the isoHbs showed significant Bohr effects in the absence of ATP. Remixing of the separated fractions resulted in an intermediate O₂ affinity (compared with the separated components), indicating the absence of functionally significant inter-

action between the individual isoHbs. Addition of ATP markedly reduced O₂ affinity and increased the Bohr effect of each of the isoHbs, allosteric behaviors that are indicative of intact tetrameric structures. The affinity-reducing effects of ATP were amplified at low pH, in accordance with the increased Hb binding of anionic phosphates under such conditions. Relative to component I, components II and III displayed low n_{50} values (0.9–1.3) in the absence and presence of ATP. The same pattern of variation in O₂ affinity among the three isoHbs was manifest at 30°C (data not shown).

Extended Hill plots of precise O₂-equilibrium curves (Figure 8) and estimates of the MWC parameters (Table 3) elucidate the mechanisms of allosteric regulatory control. In these plots, the Y-intercepts of the upper and lower asymptotes (with slopes of unity consistent with noncooperative binding of the first and last O₂ molecules) at $\log P_{O_2} = 0$ reflect the O₂ affinities of the Hb in the oxygenated and deoxygenated states, respectively.

Fitting the MWC model to the data without constraints yielded q values between 6.3 and 8.9, consistent with the existence of aggregates larger than tetramers. In accordance with the small Bohr effect that we measured in the absence of ATP (Figure 7), a reduction in pH from 7.4 to 6.9 (a range that spans intraerythrocytic conditions) only marginally affected the O₂ association constants of Hb in the T state ($\log K_T = -0.45$ and -0.54 , respectively, at 20°C with q floating). Likewise, the change in pH altered the allosteric constant: $\log L = 3.8$ and 4.3 at pH 7.4 and 6.9, respectively.

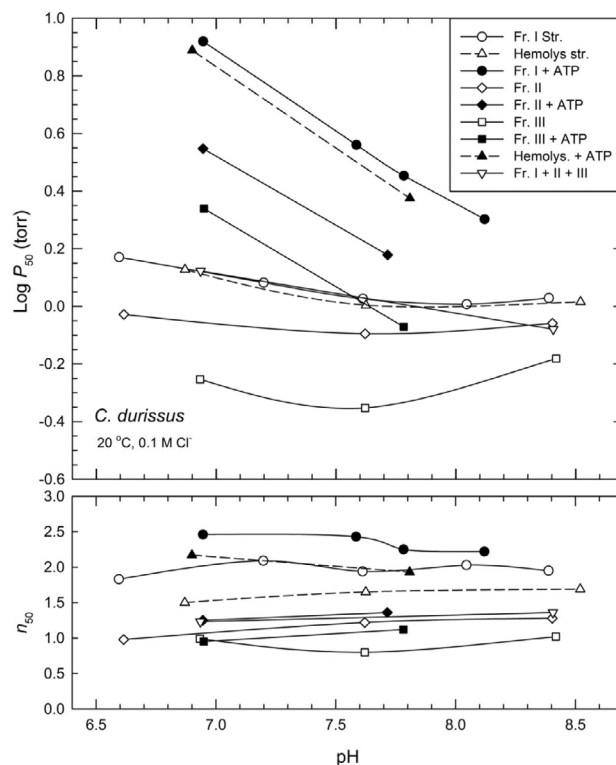


Figure 7. pH dependence of P_{50} and n_{50} values for composite hemolysate and isolated Hb components of the South American rattlesnake, *C. durissus*. O₂ affinities and cooperativities are shown for stripped (str) hemolysate (triangles), Hb fraction (Fr) I (circles), fraction II (diamonds), and fraction III (squares), and the three fractions combined in a 1:1:1 ratio (inverted triangles), in the absence (open symbols) and presence (solid symbols) of ATP. Temperature = 20°C; heme concentration 0.040 mM. Other conditions are as in Figure 6.

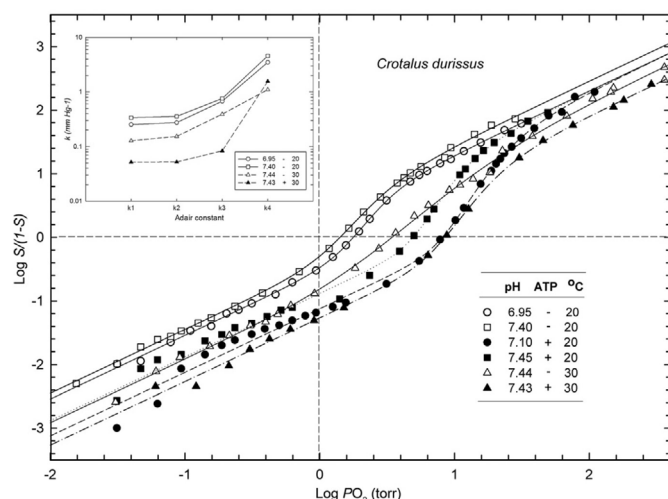


Figure 8. Extended Hill plots of stripped rattlesnake hemolysate at 20°C (circles and squares) and 30°C (triangles), in the absence (open symbols) and presence (solid symbols) of ATP, and at the indicated pH values. The inset graph shows the intrinsic Adair constants (k_1 , k_2 , k_3 , and k_4) for the four successive oxygenation steps obtained when fitting the Monod-Wyman-Changeux model to the data with freely floating values of q (the number of interacting O_2 binding sites). Other conditions are as in Figure 7.

In contrast, ATP strongly decreased K_T ($\log K_T = -0.54$ and -1.12 , at 20°C and pH ~ 7.1), without markedly changing K_R ($\log K_R = 0.30$ and 0.34 , respectively), thereby increasing the free energy of cooperative O_2 binding (from 4.74 to 8.02 kJ/mol at pH ~ 7.0), and showing that organic phosphates modulate the P_{50} of snake Hb by decreasing K_T and increasing L , as observed in other vertebrates (31, 41, 87). Phosphates analogously increased the Bohr effect of Hb in the deoxy T state (at 20°C and with q floating, $\phi_T = -0.20$ and -0.68 in the absence and presence of ATP, respectively; Figure 7). In contrast to the effects of pH and ATP, increased temperature (from 20 to 30°C) reduced K_T as well as K_R in the absence and in the presence of ATP (Table 3).

As shown in Figure 8 (inset), decreased pH and increased temperature reduce HbO_2 affinity of rattlesnake Hb via relatively uni-

form decreases in the magnitudes of the four Adair constants, whereas ATP acts mainly by reducing the binding affinities of the first, second, and third O_2 molecules, indicating that organic phosphates delay the major $T \rightarrow R$ transition until late in the oxygenation process.

Functional properties of Indian python Hbs. The stripped hemolysate of *Python molurus* exhibits extremely high O_2 affinity ($P_{50} = 1.0$ Torr at 25°C and pH 7.4), low cooperativity ($n_{50} \sim 1.5$ at pH 7.4, decreasing to ~ 1.2 at higher pH), and a small Bohr effect ($\phi = -0.17$); ATP strongly increases P_{50} , n_{50} , and the Bohr effect (Figure 9, Table 1). Of note, ATP and IHP (inositol hexaphosphate, a chemical analog of the powerful effector inositol pentaphosphate found in the red blood cells of birds and some other vertebrates) raised the ϕ more potently at phosphate-to-Hb ratios ~ 5 than at higher levels (Figure 9, inset). This phosphate dependence of the Bohr effect is explained by the fact that anionic phosphates bind to T-state Hb at low phosphate concentration, but they bind to both T- and R-state Hbs at higher phosphate concentrations (87). $\Delta H'$ was reduced in the presence of ATP (from 25.3 to 13.9 kJ/mol, assessed at pH 7.4 and 15–35°C) in accordance with the endothermic nature of oxygenation-linked ATP dissociation.

Analysis of the python data in terms of the MWC model with q floating indicates the presence of 5.9 ± 1.8 interacting O_2 -binding sites (Table 4). HbO_2 affinity is reduced at low pH because K_T is reduced while K_R remains unchanged, resulting in an increased allosteric constant L (Figure 10). The pH sensitivity of the Adair constants (Figure 10A, inset) reveal that most protons are released on oxygenation of the first two hemes ($\Delta H_i^+ = 0.26$ and 0.22 for k_1 and k_2 , respectively), whereas oxygenation of the third and fourth hemes only releases 0.12 and 0.10 protons, respectively.

Organic phosphates analogously modulate HbO_2 affinity by inducing a more stable T state (Figure 10B, Table 4), as shown by the drastic increase in the allosteric constant. At 25°C, $\log L$ increases from 1.09 in the absence of ATP to 3.26 in the presence of ATP at fivefold excess over tetrameric Hb. The Adair constants indicate that most phosphate is released on oxygenation of the first and second hemes (0.46 and 0.57 ATP molecules/bound O_2 ; Figure 10B, inset). The increased ΔG [which equals $RT \ln(K_R/K_T)$] in

Table 3. O_2 -binding and derived parameters obtained by fitting the Monod-Wyman-Changeux two-state model to O_2 -equilibrium measurements on *C. durissus* Hb

°C	pH	ATP	P_{50} , Torr	P_m , Torr	n_{50}	n_m	$\log K_T$	$\log K_R$	$\log L$	ΔG , kJ/mol	q
20	6.948	–	1.75	1.60	2.33	2.21	-0.542 ± 0.013	0.307 ± 0.022	4.28 ± 0.25	4.74	8.36 ± 0.73
20	6.948	–	1.69	1.57	1.93	1.89	-0.600 ± 0.033	0.714 ± 0.124	3.65 ± 0.49	6.41	4
20	6.948	–	1.74	1.60	2.29	2.19	-0.546 ± 0.011	0.316 ± 0.014	4.17 ± 0.10	4.80	8
20	7.403	–	1.36	1.27	2.10	2.02	-0.449 ± 0.019	0.476 ± 0.061	3.79 ± 0.28	5.09	6.50 ± 0.92
20	7.403	–	1.42	1.24	1.89	1.85	-0.474 ± 0.026	0.883 ± 0.140	3.93 ± 0.56	6.37	4
20	7.403	–	1.42	1.29	2.23	2.11	-0.437 ± 0.016	0.412 ± 0.023	4.18 ± 0.18	4.72	8
20	7.102	+	8.04	6.30	2.40	1.75	-1.122 ± 0.024	0.347 ± 0.173	8.82 ± 0.74	8.02	7.70 ± 1.93
20	7.455	+	4.87	3.81	2.37	1.68	-0.882 ± 0.033	0.314 ± 0.219	7.98 ± 0.99	6.63	8.92 ± 2.28
30	7.434	–	3.47	3.30	1.77	1.76	-0.904 ± 0.031	0.157 ± 0.069	2.72 ± 0.28	5.26	4
30	7.434	–	3.42	3.28	1.65	1.65	-0.915 ± 0.035	12.88 ± 0.852	35.4 ± 0.32	5.90	2.64 ± 0.19
30	7.430	+	8.49	7.41	2.47	2.26	-1.27 ± 0.026	-0.057 ± 0.090	5.11 ± 0.44	6.90	6.28 ± 0.98
30	7.430	+	8.21	7.30	2.12	2.03	-1.29 ± 0.033	0.598 ± 0.398	5.85 ± 1.59	8.58	4
30	7.430	+	8.66	7.42	2.72	2.35	-1.25 ± 0.024	-0.141 ± 0.039	5.83 ± 0.29	6.40	8

Values are means \pm SE. O_2 equilibria were measured at 20 or 30°C, at the indicated pH values and in the absence (–) and presence (+) of saturating ATP levels ($ATP/Hb_4 = 10.3$). P_m , median O_2 saturation; n_{50} , Hill's cooperativity coefficient at 50% saturation; n_m , median Hill cooperativity coefficient; K_R and K_T , O_2 association equilibrium constants for R-state oxygenated Hb and T-state deoxygenated Hb, respectively; L , the ratio of T- and R-state Hb in the absence of ligand; ΔG , free energy of cooperativity; q , number of interacting O_2 binding sites. The model was fitted with the number of q fixed at 4 or 8, or estimated from the model.

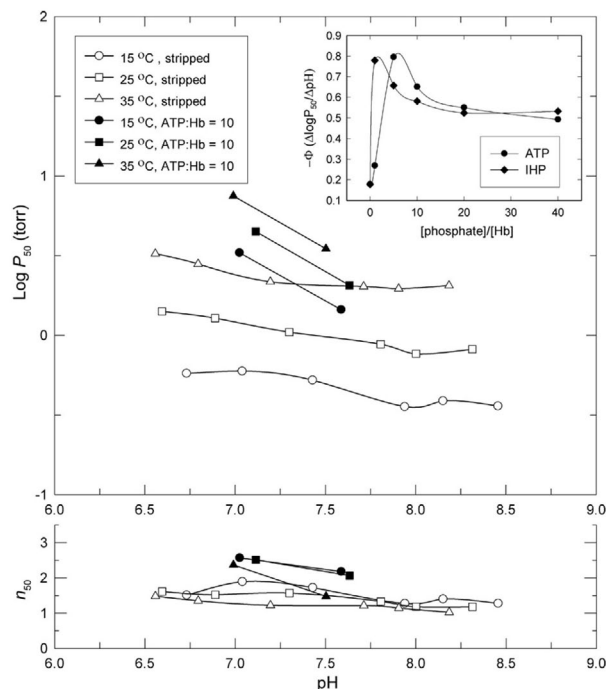


Figure 9. pH dependence of P_{50} and n_{50} values of stripped *P. molurus* Hb at 15°C (circles), 25°C (squares), and 35°C (triangles) measured in 0.1 M HEPES and 0.1 M KCl, in the absence (open symbols) and presence (solid symbols) of ATP at 10-fold molar excess over tetrameric Hb. Inset: Bohr factor at pH 7.1–7.6 and its dependence on ATP-to-Hb and GTP-to-Hb molar ratios. Heme concentration, 0.20 mM. IHP, inositol hexaphosphate.

the presence of increased ATP (Table 4) correlates with the greater phosphate sensitivity of K_T (Figure 10B).

O_2 affinity and cooperativity exhibit analogous sensitivity to Cl^- ions. Plots of $\log P_{50}$ vs. $\log [Cl^-]$ (based on P_{50} measurements at 0.05, 0.1, 0.2, and 0.5 M chloride concentrations at pH 7.1 and 7.6) (Figure 11) reveal maximum slopes of 0.23, indicating the release of 0.92 Cl^- ions upon oxygenation of the tetrameric Hb (compared with 1.6 in human Hb) (3, 79).

Similar to the case with rattlesnake Hb, the temperature sensitivity of python Hb is reduced by allosteric effectors: $\Delta H'$ was reduced from -62 kJ/mol at pH 8.2 (where the Bohr effect is absent) to -51.6 kJ/mol at pH 7.1 (where the Bohr effect is expressed). $\Delta H'$ was further reduced to -29.8 kJ/mol at pH 7.1 in the presence

of ATP (Figure 9). Increased temperature lowers K_R slightly more than K_T , thus decreasing the free energy of heme-heme interaction ($\Delta G_{pH 7.1} = 4.69$ and 3.62 kJ/mol, and 15 and 35°C, respectively) (Table 4, Figure 10C). The lower temperature effect in the deoxy state (Figure 10C) is attributable to the greater release of protons on binding of the first and second O_2 molecules than on binding the third and fourth molecules (Figure 10A).

Functional properties of yellow-bellied sea snake Hbs. The stripped, unfractionated hemolysate of the yellow-bellied sea snake exhibited a high O_2 affinity ($P_{50} = 1.2$ Torr, pH 7.4) and a small Bohr effect ($\phi = -0.17$) that was strongly increased in the presence of ATP ($\phi = -0.56$) (Table 2). In association with the low Bohr effect, the temperature sensitivity of HbO_2 affinity exhibited only slight pH dependence ($\Delta H' = -39.5$ and -37.8 kJ/mol at pH 7.4 and 8.2) (Figure 12A).

Organic phosphates strongly reduced O_2 affinity and increased cooperativity of sea snake Hb. Interestingly, GTP exerted markedly greater allosteric effects than ATP (Figure 12B). The maximum slopes of double logarithmic plots of P_{50} vs. phosphate concentration approximated 0.25, indicating 1:1 phosphate/Hb tetramer stoichiometry, as observed in Hbs of the snakes *Boa constrictor*, *Bothrops alternatus*, and *Liophis miliaris* (11), contrasting with distinctly higher slopes that reflect the binding of two anionic phosphates in Hbs of some vertebrates (59, 81, 84). In the absence of high-resolution crystal structures of the snake Hbs, it is not possible to identify additional effector binding sites.

Discussion

Characteristic Functional Properties of Snake Hbs

The Hbs of South American rattlesnake, Indian python, and yellow-bellied sea snake share a number of characteristic features, including high intrinsic O_2 affinities, low cooperativity coefficients, small ϕ values in the absence of organic phosphates, and large ATP sensitivities. Consistent with several previous studies (11, 44, 45, 69), our results suggest that snake Hbs may be generally characterized by a large capacity for regulating O_2 affinity, which may modulate tissue O_2 supply in response to changes in O_2 availability and metabolic demands. This acclimatization capacity of blood- O_2 transport provides a possible explanation for why Hbs with similar intrinsic O_2 affinities and modes of allosteric regulation appear sufficient to meet the needs of species that presumably face very dif-

Table 4. O_2 -binding and derived parameters obtained by fitting the Monod-Wyman-Changeux two-state model to O_2 -equilibrium data of *P. molurus* Hb

°C	pH	P^{n-}	$[P^{n-}]/[Hb]$	P_{50} , Torr	$P_{m'}$, Torr	n_{50}	n_m	Log K_T	Log K_R	Log L	ΔG , kJ/mol	k_1 , Torr ⁻¹	k_2 , Torr ⁻¹	k_3 , Torr ⁻¹	k_4 , Torr ⁻¹	q
25	6.60	–	–	1.48	1.59	1.60	1.59	-0.878 ± 0.083	0.098 ± 0.026	1.17 ± 0.11	4.47	0.20	0.57	1.10	1.24	4
25	7.12	–	–	1.21	1.26	1.49	1.48	-0.641 ± 0.102	0.177 ± 0.040	1.09 ± 0.18	3.71	0.33	0.68	1.22	1.45	4
25	7.72	–	–	0.93	1.01	1.38	1.36	-0.841 ± 0.151	0.180 ± 0.015	0.66 ± 0.07	3.35	0.39	1.10	1.46	1.51	4
25	8.31	–	–	0.86	0.95	1.12	1.10	-0.493 ± 0.815	0.092 ± 0.008	0.37 ± 0.80	1.80					7.7
35	7.12	–	–	3.02	3.03	1.47	1.47	-0.866 ± 0.056	-0.132 ± 0.067	1.39 ± 0.28	3.62	0.16	0.25	0.46	0.66	4
15	7.10	–	–	0.61	0.62	1.65	1.66	-0.313 ± 0.071	0.586 ± 0.046	1.52 ± 0.19	4.69	0.59	1.14	2.70	3.65	4
25	7.12	ATP	1	1.91	1.90	1.91	1.89	-0.804 ± 0.028	0.263 ± 0.035	2.17 ± 0.14	5.73	0.17	0.28	0.96	1.69	4
25	7.13	ATP	5	3.19	3.12	2.42	2.41	-1.17 ± 0.05	0.321 ± 0.072	3.26 ± 0.29	8.33	0.07	0.10	0.77	1.99	4
25	7.12	ATP	40	7.22	6.83	2.66	2.64	-1.52 ± 0.04	0.304 ± 0.131	4.56 ± 0.52	10.20	0.03	0.03	0.25	1.80	4
25	7.13	IHP	5	11.60	10.70	2.46	2.42	-1.60 ± 0.02	0.157 ± 0.185	4.75 ± 0.73	9.41	0.03	0.03	0.10	1.12	4

Values are means \pm SE. O_2 equilibria were measured at 15, 25, or 35°C, at the indicated pH values, and in the absence (–) and presence of organic phosphates (P^{n-}) at the indicated P^{n-} -to-(tetrameric) Hb ratios. The model was fitted with the q fixed at 4, except in one case where this was impossible, and q was left floating. k_1 – k_4 , intrinsic Adair constants for the four successive oxygenation steps.

ferent physiological challenges to respiratory gas transport due to differences in ecological niches (terrestrial vs. aquatic) and physical activities. For example, fully aquatic species like the yellow-bellied sea snake perform prolonged dives (68), and they rely to a large extent on cutaneous O₂ uptake (29). Both pythons and rattlesnakes exhibit pronounced metabolic increments during digestion that may exceed those measured during physical exercise (56), and the postprandial period is attended by substantial increases in

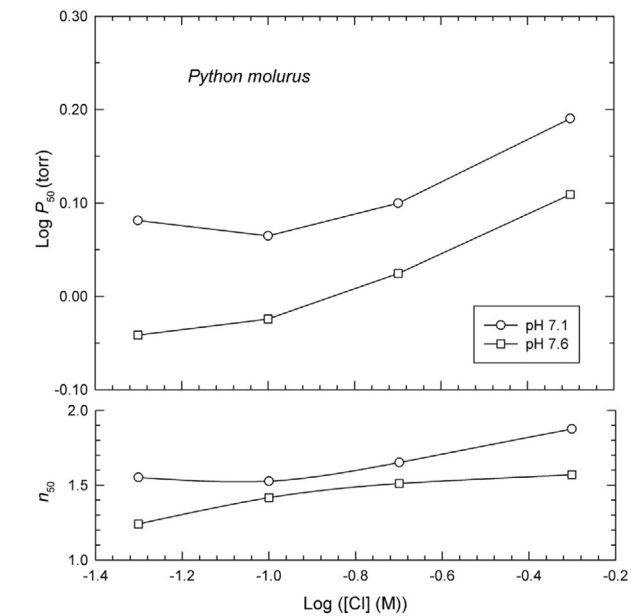
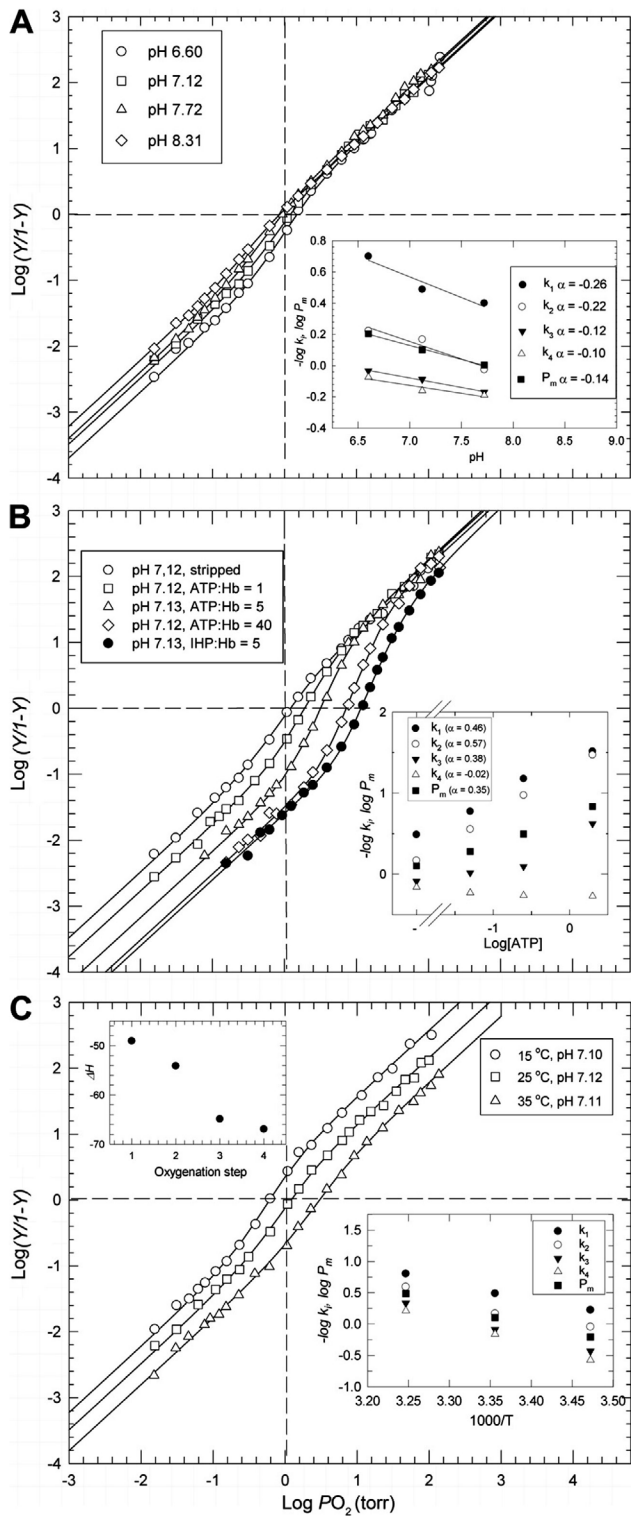


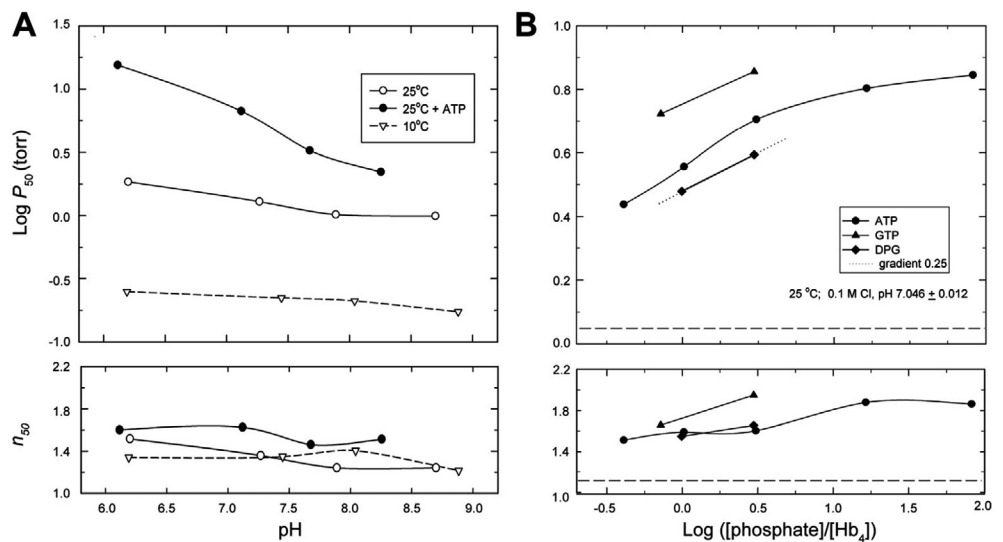
Figure 11. Effect of [Cl⁻] on the P₅₀ and n₅₀ of Indian python Hb, at pH 7.1 (○) and 7.6 (□). Other details are as in Figure 10.

blood Pco₂ and HCO₃⁻ concentrations, such that pH remains relatively constant, while plasma Cl⁻ decreases (4, 12, 57, 78). All of these changes potentially alter the O₂-binding properties of Hb. In python, postprandial changes in blood-O₂ affinity occur as a result of red cell swelling and concomitant reductions in intracellular concentrations of nucleotide triphosphates (57). In rattlesnake, by contrast, a similar postprandial increase in the blood-O₂ affinity is caused by changes in blood pH (12).

An important question is how the shared functional characteristics of snake Hbs can serve O₂ uptake and transport needs in species with such different metabolic requirements, such as aquatic species (like *P. platura*), where nonbranchial O₂ uptake requires high blood-O₂ affinities, and highly active terrestrial predators (like *C. durissus*), where high O₂ delivery rates require low blood-O₂ affinities. A crucial factor in this regard may be the large Bohr effects (ϕ ranges from -0.56 to -0.62; Table 2) that are manifest in the presence of ATP. For example, the aquatic snakes *Acrochordus javanicus* and *A. arafurae* have considerably higher blood-O₂ affinities compared with the terrestrial boa, *Boa constrictor* (P₅₀ at 20°C and pH 7.5 = ~13 vs. ~30 Torr) (70), which can be expected to aid the replenishment of blood O₂ stores, and the much larger ϕ

Figure 10. Extended Hill plots of Indian python Hbs illustrating sensitivities of O₂ affinity to pH, organic phosphates, and temperature. A: O₂ equilibria at 25°C measured at pH 6.60 (circles), 7.12 (squares), 7.72 (triangles), and 8.31 (diamonds), showing (inset) the pH dependence of the median O₂ tension (P_m) values and the Adair constants for the four oxygenation steps (k₁–k₄). B: O₂ equilibria at 25°C and pH 7.12, in the absence of phosphate effectors (open circles), in the presence of ATP [ATP-to-(tetrameric) Hb molar ratios = 1 (squares), 5 (triangles), and 40 (diamonds)], and in the presence of IHP [IHP-to-(tetrameric) Hb molar ratio = 1 (solid circles)]. Inset: P_m values and Adair constants for successive oxygenation steps in the absence of ATP (–) and at varying concentrations of ATP. C: O₂ equilibria at pH 7.11 (±0.01) measured at 15°C (circles), 25°C (squares), and 35°C (triangles), showing van't Hoff plots of the temperature dependence of k₁–k₄ and P_m (bottom inset) and the overall enthalpies (kJ/mol) for the four oxygenation steps (top inset). Other experimental conditions: 0.1 M HEPES buffer, 0.1 M KCl, 0.2 M heme concentration.

Figure 12. Effects of pH, temperature, and organic phosphates on O₂ binding by sea snake (*P. platura*) Hb. **A:** P₅₀ and n₅₀ values at 10°C (inverted triangles) and 2°C (circles) in the absence (open symbols) and presence (solid symbols) of saturating concentrations of ATP [ATP-to-Hb (tetramer) ratio: ~80]. **B:** effects of ATP (circles), GTP (triangles), and 2,3-diphosphoglycerate (DPG; diamonds) at pH 7.05 and 25°C, where the horizontal dashed lines show P₅₀ and n₅₀ values in the absence of the phosphate effectors, and the dotted line shows a gradient of 0.25 (that reflects binding of one phosphate molecule per Hb tetramer). Other experimental conditions: 0.1 M HEPES and 0.1 M KCl, heme concentration 0.32 M.



values ($\phi = -1.0$ to -1.47 in the aquatic species vs. -0.4 in the boa) should help compensate for the inherently high O₂ affinity in promoting O₂ release in the active tissues (42). However, data from sea snakes demonstrate that large Bohr shifts are not uniquely associated with diving (70).

What Structural and Functional Mechanisms Account for the High O₂ Affinity, Low Cooperativity, and Distinctive Modes of Allosteric Regulation of Snake Hbs?

Known phosphate-binding sites (basic amino acid residues at β -chain positions 2, 81, 143, and 146) are conserved in most snake Hbs, although $\beta 143\text{His}$ has been substituted for Arg or Tyr in the β' -globins of numerous species (Figure 1B). Surprisingly, our O₂ affinity measurements revealed high phosphate sensitivities in the Hbs of South American rattlesnake, Indian python, and yellow-bellied sea snake (Table 2), despite the fact that the highly conserved $\beta 2\text{His}$ is replaced by Asn and Gln in the β'' -globins of python and rattlesnake, respectively (Figure 1B). The high ATP sensitivities of snake Hbs (Table 2) are consistent with the finding that deoxy-Hbs of *Liophis miliaris*, *Boa constrictor*, and *Bothrops alternatus* have higher ATP association constants relative to human Hb. In the case of *L. miliaris* Hb, Bonilla et al. (11) suggested that the high affinity for ATP-binding is mainly attributable to $\beta 3\text{Trp}$ (which increases hydrophobicity, relative to $\beta 3\text{Leu}$ in human Hb) and $\beta 101\text{Val}$ (a polar \rightarrow nonpolar change relative to $\beta 101\text{Glu}$ in human Hb). The reduced Cl⁻ sensitivity of python Hb may be partly attributable to the substitution of nonpolar Met for polar Ser at $\alpha^D 131\text{Ser}$ (Figure 1A), a known chloride-binding site in vertebrate Hb (90).

In addition to ATP, the predominant nucleoside triphosphate found in ectothermic vertebrates, snake red cells contain substantial concentrations of GTP (6, 54). The markedly greater sensitivity of sea snake Hb to GTP than ATP (Figure 12B) corresponds with findings for fish Hbs (88), where stereochemical complementarity of the phosphate binding site to strain-free nucleoside triphosphates results from $\beta 2\text{His} \rightarrow \text{Glu/Asp}$ and $\beta 143\text{His} \rightarrow \text{Arg}$ substitutions (compared with most vertebrate Hbs) and GTP binds by an additional hydrogen bond compared with ATP (32). Of note, $\beta 2$ and

$\beta 143$ residues are also substituted in python Hb (by nonpolar, neutral Asn and Gln residues, respectively; Figure 1B).

The Bohr effect of stripped rattlesnake Hb (-0.21) is greater than that seen in the Hbs of the relatively less active python and sea snake (-0.17 in both species) (Table 2). Given that the COOH-terminal His residues contribute about one-half of the maximal alkaline Bohr effect expressed by human Hb in 0.1 M NaCl (8), the low Bohr effect of sea snake Hb is consistent with the $\beta 146\text{His} \rightarrow \text{Tyr}$ substitution reported for its major isoHb (43).

Can Oxygenation Properties of Snake Hbs be Explained by Allosteric Transitions in the Quaternary Structure of Intact Tetramers?

Even at the low Hb concentrations used in our in vitro experiments, oxygenation properties of Hbs from each of the three snake species that we examined could be explained entirely by allosteric R \leftrightarrow T transitions of intact tetramers. Our results for South American rattlesnake Hbs are consistent with previous studies of Hb in this same species (44, 45) and suggest that reversible, oxygenation-linked dissociation of Hb tetramers into $\alpha\beta$ -dimers is not a universal feature of snake Hbs under in vitro or in vivo conditions. Previous studies demonstrated that *C. durissus* Hb remains in mostly tetrameric form, even at concentrations of 1 mM (45).

However, results of the gel filtration experiments demonstrate that python Hbs exhibit a greater tendency to dissociate in vitro than those of rattlesnake. Thus, whereas rattlesnake Hb is predominantly tetrameric in the oxygenated state and aggregates to larger complexes on deoxygenation, python Hb is predominantly tetrameric when deoxygenated and undergoes reversible dissociation to dimers and monomers when ligated. Interestingly, the presence of ATP distinctly augments aggregation of python Hb, resulting in predominantly tetrameric structures in the CO-ligated state and higher order aggregates in the deoxygenated state. This is consistent with the reported ATP-induced tetramerization observed in *H. modestus* Hb at low concentration (0.08–0.14 mM as heme) (9). Moreover, aggregation of rattlesnake and python Hbs is indicated by estimated q values >4 when the O₂-equilibrium data were fit to the MWC model.

What is the Nature of isoHb Differentiation, and Is the Isoform Repertoire of Snakes Qualitatively Similar to That of Other Amniote Vertebrates?

Adult specimens of *Boa constrictor* express two main isoHbs that exhibit highly similar functional properties at high phosphate concentrations (69). By contrast, our experiments on isolated isoHbs of the South American rattlesnake revealed appreciable differences in O₂ affinity over a wide pH range, and the magnitude of the affinity differences was consistent in the presence and absence of ATP. The additive effects of the individual isoHbs on the O₂ affinity of the composite hemolysate (Figure 7) are consistent with previous studies of *C. durissus* Hbs (44, 45) and are also consistent with remixing experiments involving the HbA and HbD isoforms of birds (31, 91).

Surprisingly, the major isoHb of the South American rattlesnake is homologous to “HbD” of other amniote vertebrates in that the α -type subunits are encoded by orthologous α^D -globin genes (the adult-expressed β -globin genes of snakes are not 1:1 orthologs of those of other amniotes) (38, 72). In the case of turtles and birds, HbA is always the major isoform, and HbD is always the minor isoform (15, 17, 27, 31, 55, 61). Moreover, in all turtle and bird species that have been examined, HbD exhibits a consistently higher O₂ affinity than HbA, in both the presence and absence of anionic effectors (15, 17, 27, 31, 33, 34, 61). Remarkably, isoHb differentiation in the South American rattlesnake shows the exact opposite pattern: HbD (= component I) is the major isoform, and it has a uniformly lower O₂ affinity than HbA over all treatment conditions (Figure 7). The finding that HbD is the major isoHb in rattlesnake is consistent with data on isoHb composition in the green anole lizard, *Anolis carolinensis* (72), and suggests the possibility that HbD represents the major adult isoHb in squamate reptiles in general. In all sauropsid taxa that have been examined to date, it is intriguing that the minor adult isoHb (HbA in snakes, HbD in turtles and birds) consistently has a higher O₂ affinity than the corresponding major isoHb, even when the identities of major and minor isoHbs are reversed in different taxa. Experimental data from additional squamate reptiles will be required to assess the generality of this pattern.

Perspectives and Significance

The fact that these ecologically and physiologically distinct snake species have Hbs with such similar respiratory properties suggests that regulatory control of O₂-transport may be vested at higher levels of biological organization and may involve changes in the cellular concentrations of allosteric effectors and/or changes in various systemic factors that govern O₂ flux from the respiratory surfaces to the mitochondria (ventilation rate, cardiac output, capillary densities, and physical properties of diffusion barriers at sites of O₂ loading and unloading). Alternatively, a lack of interspecific variation in aerobic capacities may reflect the fact that many activities are supported by transient increases in anaerobic metabolism.

Grants — The authors acknowledge grant support from the National Science Foundation (NSF IOS-1354390 and MCB-1517636; J. F. Storz), the National Heart, Lung, and Blood Institute (HL-087216; J. F. Storz), the Danish Council for In-

dependent Research, Natural Sciences (10-084-565; A. Fago), and the Faculty of Science and Technology, Aarhus University (R. E. Weber).

Disclosures — No conflicts of interest, financial or otherwise, are declared by the authors.

Author contributions — J.F.S., C.N., H.M., F.G.H., T.W., A.F., H.M., J.O., and R.E.W. analyzed data; J.F.S., F.G.H., T.W., A.F., H.M., J.O., and R.E.W. interpreted results of experiments; J.F.S., C.N., F.G.H., J.O., and R.E.W. prepared figures; J.F.S. and R.E.W. drafted manuscript; J.F.S., C.N., T.W., A.F., H.M., J.O., and R.E.W. edited and revised manuscript; J.F.S., C.N., H.M., F.G.H., T.W., A.F., H.M., J.O., and R.E.W. approved final version of manuscript; J.F.S., J.O., and R.E.W. conception and design of research; C.N., H.M., and T.W. performed experiments.

Acknowledgments — The authors thank the associate editor and reviewers for *American Journal of Physiology — Regulatory, Integrative and Comparative Physiology* for helpful suggestions that improved the manuscript.

References

1. Ackers GK. Molecular exclusion and restricted diffusion processes in molecular-sieve chromatography. *Biochemistry* 3: 723–730, 1964.
2. Adair GS. The hemoglobin system. VI. The oxygen dissociation curve of hemoglobin. *J Biol Chem* 63: 529–545, 1925.
3. Amiconi G, Antonini E, Brunori M, Wyman J, Zolla L. Interaction of hemoglobin with salts. Effects on the functional properties of human hemoglobin. *J Mol Biol* 152: 111–129, 1981.
4. Arvedsen SK, Andersen JB, Zaar M, Andrade D, Abe AS, Wang T. Arterial acid-base status during digestion and following vascular infusion of NaHCO₃ and HCl in the South American rattlesnake, *Crotalus durissus*. *Comp Biochem Physiol A* 142: 495–502, 2005.
5. Baldwin J, Chothia C. Haemoglobin: The structural changes related to ligand binding and its allosteric mechanism. *J Mol Biol* 129: 175–220, 1979.
6. Bartlett GR. Phosphate compounds in vertebrate red blood cells. *Am Zool* 20: 103–114, 1980.
7. Bellelli A, Brunori M, Miele AE, Panetta G, Vallone B. The allosteric properties of hemoglobin: Insights from natural and site directed mutants. *Curr Protein Pept Sci* 7: 17–45, 2006.
8. Berenbrink M. Evolution of vertebrate haemoglobins: Histidine side chains, specific buffer value and Bohr effect. *Respir Physiol Neurobiol* 154: 165–184, 2006.
9. Bonafé CFS, Matsukuma AY, Matsuura MSA. ATP-induced tetramerization and cooperativity in hemoglobin of lower vertebrates. *J Biol Chem* 274: 1196–1198, 1999.
10. Bonilla GO, Focesi A Jr, Bonaventura C, Bonaventura J, Cashon RE. Functional properties of the hemoglobin from the South American snake *Mastigodryas bifossatus*. *Comp Biochem Physiol A* 109: 1085–1095, 1994.
11. Bonilla GO, Oyama S Jr, Nagatomo CL, Matsuura MSA, Focesi A Jr. Interactions of adenosine triphosphate with snake hemoglobins. Studies in *Liophis miliaris*, *Boa constrictor* and *Bothrops alternatus*. *Comp Biochem Physiol B* 109: 701–707, 1994.
12. Bovo RP, Fuga A, Micheli-Campbell MA, Carvalho JE, Andrade DV. Blood oxygen affinity increases during digestion in the South American rattlesnake, *Crotalus durissus terrificus*. *Comp Biochem Physiol A* 186: 75–82, 2015.
13. Brittain T. Cooperativity and allosteric regulation in non-mammalian vertebrate haemoglobins. *Comp Biochem Physiol B* 99: 731–740, 1991.
14. Brunori M, Giardina B, Chiancone E, Spagnuolo C, Binotti I, Antonini E. Studies on the properties of fish hemoglobins. Molecular properties and interaction with third components of the iso-

- lated hemoglobins from trout (*Salmo irideus*). *Eur J Biochem* 39: 563–570, 1973.
15. **Cheviron ZA, Natarajan C, Projecto-Garcia J, Eddy DK, Jones J, Carling MD, Witt CC, Moriyama H, Weber RE, Fago A, Storz JF.** Integrating evolutionary and functional tests of adaptive hypotheses: A case study of altitudinal differentiation in hemoglobin function in an Andean sparrow, *Zonotrichia capensis*. *Mol Biol Evol* 31: 2948–2962, 2014.
 16. **Chiancon E.** Dissociation of hemoglobin into subunits. II. Human oxyhemoglobin: Gel filtration studies. *J Biol Chem* 267: 1212–1219, 1968.
 17. **Damsgaard C, Storz JF, Hoffmann FG, Fago A.** Hemoglobin isoform differentiation and allosteric regulation of oxygen binding in the turtle, *Trachemys scripta*. *Am J Physiol Regul Integr Comp Physiol* 305: R961–R967, 2013.
 18. **Duguet M, Acher R.** The oxygen dissociation curve of viper (*Vipera aspis*) hemoglobin: Functional similarity with human hemoglobin Portland. *FEBS Lett* 60: 267–268, 1975.
 19. **Edgar RC.** MUSCLE: Multiple sequence alignment with high accuracy and high throughput. *Nucleic Acids Res* 32: 1792–1797, 2004.
 20. **Eguchi T, Eguchi Y.** Amino acid sequence of the α - and β -globin chains of the Erabu sea snake (*Laticauda semifasciata*). *J Protein Chem* 22: 489–497, 2003.
 21. **Eguchi Y, Eguchi T.** Amino acid sequence of the α - and β -globin chains of the Hiroo sea snake (*Laticauda laticaudata*). *J Protein Chem* 21: 215–221, 2002.
 22. **Fago A, Bendixen E, Malte H, Weber RE.** The anodic hemoglobin of *Anguilla anguilla*. Molecular basis for allosteric effects in a root-effect hemoglobin. *J Biol Chem* 272: 15628–15635, 1997.
 23. **Fago A, Romano M, Tamburrini M, Coletta M, D'Avino R, Di-Prisco G.** A polymerising Root-effect fish hemoglobin with high subunit heterogeneity. Correlation with primary structure. *Eur J Biochem* 218: 829–835, 1993.
 24. **Focesi A Jr, Bonilla GO, Nagatomo CL, Matsuura MSA.** Dimertetramer transition in hemoglobin from *Liophis miliaris*. III. The phenomenon in snake species of different evolutionary levels. *Comp Biochem Physiol B* 103: 985–989, 1992.
 25. **Focesi A Jr, Ogo SH, Matsuura MSA.** Dimer-tetramer transition in hemoglobins from *Liophis miliaris*. II. Evidence with the stripped proteins. *Comp Biochem Physiol B* 96: 119–122, 1990.
 26. **Focesi A Jr, Ogo SH, Matsuura MSA, Say JC.** Further evidence of dimer-tetramer transition in hemoglobin from *Liophis miliaris* Braz. *J Med Biol Res* 20: 861–864, 1987.
 27. **Galen SC, Natarajan C, Moriyama H, Weber RE, Fago A, Benham PM, Chavez AN, Cheviron ZA, Storz JF, Witt CC.** Contribution of a mutational hot spot to hemoglobin adaptation in high-altitude Andean house wrens. *Proc Natl Acad Sci USA*. In press.
 28. **Gorr TA, Mable BK, Kleinschmidt T.** Phylogenetic analysis of reptilian hemoglobins: trees, rates, and divergences. *J Mol Evol* 47: 471–485, 1993.
 29. **Graham JB.** Aquatic respiration in the sea snake *Pelamis platurus*. *Respir Physiol* 21: 1–7, 1974.
 30. **Graham JB, Rubinoff I, Hecht MK.** The respiratory consequences of feeding in amphibians and reptiles. *Proc Natl Acad Sci USA* 68: 1360–1363, 1971.
 31. **Grispo MT, Natarajan C, Projecto-Garcia J, Moriyama H, Weber RE, Storz JF.** Gene duplication and the evolution of hemoglobin isoform differentiation in birds. *J Biol Chem* 287: 37647–37658, 2012.
 32. **Gronenborn AM, Clore GM, Brunori M, Giardina B, Falcioni G, Perutz MF.** Stereochemistry of ATP and GTP bound to fish haemoglobins. A transferred nuclear Overhauser enhancement, 31P-nuclear magnetic resonance, oxygen equilibrium and molecular modelling study. *J Mol Biol* 178: 731–742, 1984.
 33. **Hiebl I, Weber RE, Schneegans D, Braunitzer G.** High-altitude respiration of Falconiformes: The primary structures and functional properties of the major and minor hemoglobin components of the adult white-headed vulture (*Trigonoceps occipitalis*, Aegypiinae). *Biol Chem Hoppe Seyler* 370: 699–706, 1989.
 34. **Hiebl I, Weber RE, Schneegans D, Kusters J, Braunitzer G.** High-altitude respiration of birds. Structural adaptations in the major and minor hemoglobin components of adult Rüppell's griffon (*Gyps rueppellii*): A new molecular pattern for hypoxia tolerance. *Biol Chem Hoppe Seyler* 369: 217–232, 1988.
 35. **Hoffmann FG, Opazo JC, Storz JF.** Differential loss and retention of cytoglobin, myoglobin, and globin-E during the radiation of vertebrates. *Genome Biol Evol* 3: 588–600, 2011.
 36. **Hoffmann FG, Opazo JC, Storz JF.** Whole-genome duplications spurred the functional diversification of the globin gene superfamily in vertebrates. *Mol Biol Evol* 29: 303–312, 2012.
 37. **Hoffmann FG, Storz JF.** The α^D -globin gene originated via duplication of an embryonic α -like globin gene in the ancestor of tetrapod vertebrates. *Mol Biol Evol* 24: 1982–1990, 2007.
 38. **Hoffmann FG, Storz JF, Gorr TA, Opazo JC.** Lineage-specific patterns of functional diversification in the α - and β -globin gene families of tetrapod vertebrates. *Mol Biol Evol* 27: 1126–1138, 2010.
 39. **Imai K.** *Allosteric Effects in Haemoglobin*. Cambridge, UK: Cambridge University Press, 1982.
 40. **Ingermann RL.** Vertebrate hemoglobins. *Handbook of Physiology. Comparative Physiology*. Bethesda, MD: Am. Physiol. Soc., 1997, sect. 13, vol. I, chapt. 6, p. 357–408.
 41. **Jensen FB, Weber RE.** Thermodynamic analysis of precisely measured oxygen equilibria of tench (*Tinca tinca*) hemoglobin and their dependence on ATP and protons. *Comp Biochem Physiol B* 157: 137–143, 1987.
 42. **Johansen K, Lenfant C.** A comparative approach to the adaptability of O₂-Hb affinity. In: *Oxygen Affinity of Hemoglobin and Red Cell Acid-Base Status*, edited by Astrup P & Rørth M. Copenhagen: Munksgaard, 1972, p. 750–780.
 43. **Liu CS.** Preparation and chemical characterization of the three chains of the major hemoglobin of the sea snake, *Pelamis platurus*. *J Biochem* 78: 19–29, 1975.
 44. **Lombardi FR, Anazetti MC, Santos GC, Olivieri JR, Filgueira de Azevedo W Jr, Bonilla-Rodriguez GO.** Rattlesnake hemoglobins: Functional properties and tetrameric stability. *Protein Pept Lett* 13: 517–523, 2006.
 45. **Lombardi FR, Anazetti MC, Santos GC, Polizelli PP, Olivieri JR, Filgueira de Azevedo W Jr, Bonilla-Rodriguez GO.** Oxygen binding properties and tetrameric stability of hemoglobins from the snakes *Crotalus durissus terrificus* and *Liophis miliaris*. In: *Frontiers in Protein and Peptide Sciences*, edited by Dunn BM. Beijing: Bentham, 2014, p. 3–30.
 46. **Manning LR, Jenkins WT, Hess JR, Vandegriff K, Winslow RM, Manning JM.** Subunit dissociations in natural and recombinant hemoglobins. *Protein Sci* 5: 775–781, 1996.
 47. **Matsuura MSA, Ogo SH, Focesi A Jr.** Dimer-tetramer transition in haemoglobins from *Liophis miliaris*. I. Effect of organic phosphates. *Comp Biochem Physiol A* 86: 683–687, 1987.
 48. **Milsom WK.** Intermittent breathing in vertebrates. *Annu Rev Physiol* 53: 87–105, 1991.
 49. **Monod J, Wyman J, Changeux JP.** On the nature of allosteric transitions: A plausible model. *J Mol Biol* 12: 88–118, 1965.
 50. **Natarajan C, Jiang X, Fago A, Weber RE, Moriyama H, Storz JF.** Expression and purification of recombinant hemoglobin in *Escherichia coli*. *PLoS One* 6: e20176, 2011.
 51. **Natarajan C, Hoffmann FG, Lanier HC, Wolf CJ, Cheviron ZA, Spangler ML, Weber RE, Fago A, Storz JF.** Intraspecific polymorphism, interspecific divergence, and the origins of function-altering mutations in deer mouse hemoglobin. *Mol Biol Evol* 32: 978–997, 2015.
 52. **Nikinmaa M.** Haemoglobin function in vertebrates: Evolutionary changes in cellular regulation in hypoxia. *Respir Physiol* 128: 317–329, 2001.
 53. **Ogo SH, Abe AS, Focesi A Jr.** Oxygen dissociation constants in haemoglobins of *Helicops modestus* and *Liophis miliaris*, two water-snakes with different morphological adaptations to their aquatic environment. *Comp Biochem Physiol A* 63: 285–289, 1979.
 54. **Ogo SH, Matsuura MSA, Focesi A Jr.** Content of organic polyphosphates and their allosteric effects on haemoglobins from the water-snakes *Helicops modestus* and *Liophis miliaris*. *Comp Biochem Physiol A* 78: 587–589, 1984.
 55. **Opazo JC, Hoffman FG, Natarajan C, Witt CC, Berenbrink M, Storz JF.** Gene turnover in the avian globin gene family and evo-

- lutionary changes in hemoglobin isoform expression. *Mol Biol Evol* 32: 871–887, 2015.
56. **Overgaard J, Busk M, Hicks JW, Jensen FB, Wang T.** Respiratory consequences of feeding in the snake *Python molorus*. *Comp Biochem Physiol A* 124: 359–365, 1999.
 57. **Overgaard J, Wang T.** Increased blood oxygen affinity during digestion in the snake *Python molorus*. *J Exp Biol* 53: 3327–3334, 2002.
 58. **Oyama S Jr, Nagatomo CL, Bonilla GO, Matsuura MSA, Focesi A Jr.** *Bothrops alternatus* hemoglobin components. Oxygen binding properties and globin chain hydrophobic analysis. *Comp Biochem Physiol B* 105: 271–275, 1993.
 59. **Pellegrini M, Giardina B, Verde C, Carratore V, Olanas A, Sollai L, Sann MT, Castagnola M, Di Prisco G.** Structural-functional characterization of the cathodic haemoglobin of the conger eel *Conger conger*: Molecular modelling study of an additional phosphate-binding site. *Biochem J* 372: 679–686, 2003.
 60. **Perutz MF.** Stereochemistry of cooperative effects in haemoglobin. *Nature* 228: 726–739, 1970.
 61. **Projecto-Garcia J, Natarajan C, Moriyama H, Weber RE, Fago A, Cheviron ZA, Dudley R, McGuire JA, Witt CC, Storz JF.** Repeated elevational transitions in hemoglobin function during the evolution of Andean hummingbirds. *Proc Natl Acad Sci USA* 110: 20669–20674, 2013.
 62. **Ragsdale FR, Herman JK, Ingermann RL.** Nucleotide triphosphate levels versus oxygen affinity of rattlesnake red cells. *Respir Physiol* 102: 63–69, 1995.
 63. **Ragsdale FR, Imel KM, Nilsson EE, Ingermann RL.** Pregnancy-associated factors affecting organic phosphate levels and oxygen affinity of garter snake red cells. *Gen Comp Endocrinol* 91: 181–188, 1993.
 64. **Ragsdale FR, Ingermann RL.** Influence of pregnancy on the oxygen affinity of red cells from the northern Pacific rattlesnake *Crotalus viridis oreganus*. *J Exp Biol* 159: 501–505, 1991.
 65. **Rapoport S, Guest GM.** Distribution of acid-soluble phosphorus in the blood cells of various vertebrates. *J Biol Chem* 138: 269–282, 1941.
 66. **Revsbech IG, Tufts DM, Projecto-Garcia J, Moriyama H, Weber RE, Storz JF, Fago A.** Hemoglobin function and allosteric regulation in semi-fossorial rodents (family Sciuridae) with different altitudinal ranges. *J Exp Biol* 216: 4264–4271, 2013.
 67. **Ruben JA.** Aerobic and anaerobic metabolism during activity in snakes. *Comp Biochem Physiol B* 109: 147–157, 1976.
 68. **Rubinoff I, Graham JB, Motta J.** Diving of the sea snake *Pelamis platurus* in the Gulf of Panamá. I. Diving depth and duration. *Mar Biol* 91: 181–191, 1986.
 69. **Schwantes A, Schwantes ML, Bonaventura C, Sullivan B, Bonaventura J.** Hemoglobins of *Boa constrictor amarali*. *Comp Biochem Physiol B* 54: 447–450, 1976.
 70. **Seymore RS, Dobson GP, Baldwin J.** Respiratory and cardiovascular physiology of the aquatic snake, *Acrochordus arafurae*. *J Comp Physiol* 144: 215–227, 1981.
 71. **Standaert T, Johansen K.** Cutaneous gas-exchange in snakes. *J Comp Physiol* 89: 313–320, 1974.
 72. **Storz JF, Hoffmann FG, Opazo JC, Sanger TJ, Moriyama H.** Developmental regulation of hemoglobin synthesis in the green anole lizard *Anolis carolinensis*. *J Exp Biol* 214: 575–581, 2011.
 73. **Storz JF, Opazo JC, Hoffmann FG.** Gene duplication, genome duplication, and the functional diversification of vertebrate globins. *Mol Phylogenet Evol* 66: 469–478, 2013.
 74. **Storz JF, Opazo JC, Hoffmann FG.** Phylogenetic diversification of the globin gene superfamily in chordates. *IUBMB Life* 63: 313–322, 2011.
 75. **Storz JF, Weber RE, Fago A.** Oxygenation properties and oxidation rates of mouse hemoglobins that differ in reactive cysteine content. *Comp Biochem Physiol A* 161: 265–270, 2012.
 76. **Sullivan B.** Oxygenation properties of snake hemoglobins. *Science* 157: 1308–1310, 1967.
 77. **Tamura K, Stecher G, Peterson D, Filipowski A, Kumar S.** MEGA6: Molecular Evolutionary Genetics Analysis Version 6.0. *Mol Biol Evol* 30: 2725–2729, 2013.
 78. **Wang T, Busk M, Overgaard J.** The respiratory consequences of feeding in amphibians and reptiles. *Comp Biochem Physiol A* 128: 535–549, 2001.
 79. **Weber RE.** Use of ionic and zwitterionic (tris bistris and HEPES) buffers in studies on hemoglobin function. *J Appl Physiol* 72: 1611–1615, 1992.
 80. **Weber RE, Campbell KL.** Temperature dependence of haemoglobin-oxygen affinity in heterothermic vertebrates: Mechanisms and biological significance. *Acta Physiol (Oxf)* 202: 549–562, 2011.
 81. **Weber RE, Campbell KL, Fago A, Malte H, Jensen FB.** ATP-induced temperature independence of hemoglobin-O₂ affinity in heterothermic billfish. *J Exp Biol* 213: 1579–1585, 2010.
 82. **Weber RE, Fago A.** Functional adaptation and its molecular basis in vertebrate hemoglobins, neuroglobins and cytoglobins. *Respir Physiol Neurobiol* 144: 141–159, 2004.
 83. **Weber RE, Fago A, Campbell KL.** Enthalpic partitioning of the reduced temperature sensitivity of O₂-binding in bovine hemoglobin. *Comp Biochem Physiol A* 176: 20–25, 2014.
 84. **Weber RE, Fago A, Malte H, Storz JF, Gorr TA.** Lack of conventional oxygen-linked proton and anion binding sites does not impair allosteric regulation of oxygen binding in dwarf caiman hemoglobin. *Am J Physiol Regul Integr Comp Physiol* 305: R300–R312, 2013.
 85. **Weber RE, Fago A, Val AL, Bang A, Van Hauwaert ML, Dewilde S, Zal F, Moens L.** Isohemoglobin differentiation in the bimodal-breathing amazon catfish *Hoplosternum littorale*. *J Biol Chem* 275: 17297–17305, 2000.
 86. **Weber RE, Jensen FB.** Functional adaptations in hemoglobins from ectothermic vertebrates. *Annu Rev Physiol* 50: 161–179, 1988.
 87. **Weber RE, Jensen FB, Cox RP.** Analysis of teleost hemoglobin by Adair and Monod-Wyman-Changeux models — Effects of nucleoside triphosphates and pH on oxygenation of tench hemoglobin. *Comp Biochem Physiol B* 157: 145–152, 1987.
 88. **Weber RE, Lykkeboe G.** Respiratory adaptations in carp blood. Influences of hypoxia, red cell organic phosphates, divalent cations and CO₂ on hemoglobin-oxygen affinity. *J Comp Physiol B* 128: 127–137, 1978.
 89. **Weber RE, Malte H, Braswell EH, Oliver RWA, Green BN, Sharma PK, Kuchumov A, Vinogradov SN.** Mass-spectrometric composition, molecular mass and oxygen-binding of *Macrobrachium deccan* hemoglobin and its tetramer and monomer subunits. *J Mol Biol* 251: 703–720, 1995.
 90. **Weber RE, Ostojic H, Fago A, Dewilde S, Van Hauwaert ML, Moens L, Monge C.** Novel mechanism for high-altitude adaptation in hemoglobin of the Andean frog *Telmatobius peruvianus*. *Am J Physiol Regul Integr Comp Physiol* 283: R1052–R1060, 2002.
 91. **Weber RE, Voelter W, Fago A, Echner H, Campanella E, Low PS.** Modulation of red cell glycolysis: Interactions between vertebrate hemoglobins and cytoplasmic domains of band 3 red cell membrane proteins. *Am J Physiol Regul Integr Comp Physiol* 287: R454–R464, 2004.
 92. **Wells RMG.** Evolution of haemoglobin function: Molecular adaptations to environment. *Clin Exp Pharmacol Physiol* 26: 591–595, 1999.
 93. **Wyman J.** Linked functions and reciprocal effects in hemoglobin—a 2nd look. *Adv Protein Chem* 19: 223–286, 1964.
 94. **Zhang G, Li C, Li Q, Li B, Larkin DM, Lee C, Storz JF, Antunes A, Greenwold MJ, Meredith RW, Odeen A, Cui J, Zhou Q, Xu L, Pan H, Wang Z, Jin L, Zhang P, Hu H, Yang W, Hu J, Xiao J, Yang Z, Liu Y, Xie Q, Yu H, Lian J, Wen P, Zhang F, Li H, Zeng Y, Xiong Z, Liu S, Zhou L, Huang Z, An N, Wang J, Zheng Q, Xiong Y, Wang G, Wang B, Wang J, Fan Y, da Fonseca RR, Alfaro-Nunez A, Schubert M, Orlando L, Mourier T, Howard JT, Ganapathy G, Pfenning A, Whitney O, Rivas MV, Hara E, Smith J, Farre M, Narayan J, Slavov G, Romanov MN, Borges R, Machado JP, Khan I, Springer MS, Gatesy J, Hoffmann FG, Opazo JC, Hastad O, Sawyer RH, Kim H, Kim KW, Kim HJ, Cho S, Li N, Huang Y, Bruford MW, Zhan X, Dixon A, Bertelsen MF, Derryberry E, Warren W, Wilson RK, Li S, Ray DA, Green RE, O'Brien SJ, Griffin D, Johnson WE, Haussler D, Ryder OA, Willerslev E, Graves GR, Alstroem P, Fjeldsa J, Mindell DP, Edwards SV, Braun EL, Rahbek C, Burt DW, Houde P, Zhang Y, Yang H, Wang J; Avian Genome Consortium, Jarvis ED, Gilbert MT, Wang J.** Comparative genomics reveals insights into avian genome evolution and adaptation. *Science* 346: 1311–1320, 2014.